Norwegian University of Life Sciences

Master's Thesis 2019 30 ECTS
Faculty of Science and Technology

Retention of Microplastic Particles in Road Side Ditches

Tilbakeholdelse av mikroplast I veigrøft

Ingvild Darbo
Master of Science in Water and Environmental Engineering

Happiness can be found, even in the darkest of times,
if one only remembers to turn on the light.

Albus Percival Wulfric Brian Dumbledore (1881–1997)

Acknowledgements

This master thesis marks the end of a two-year master's programme at the Norwegian University of Life Sciences (NMBU). It is written for the Faculty of Science and Technology in Ås in the spring of 2019, and is worth 30 ECTS.

I would like to dedicate this thesis to my farmor, Eva Darbo-Nordgaard. You were always my biggest fan, and I would not be where I am without you.

Firstly, I would like to give a big thanks to my supervisor Vegard Nilsen for all his help and invested time. Without you this project would never have been completed. Thank you also to Sven Andreas Högfeldt, for all your help in the lab. I would also like to thank Arve Heistad, Demmelash Mengistu, Lene Hermansen, Tore Krogstad, Lars Molstad and Lars Buhler for their help throughout this semester. Lastly, thank you to my fellow students in study room 120 for countless cake-fridays and for the good times.

Ås, June 2019

Ingvild Darbo

Summary

This thesis is about microplastics. The first part studies at the possibility of using fluorescent staining as a method for identifying and quantifying microplastics from car tyres. Part two examines the ability of different ditch materials to retain microplastic. Here materials from the existing road ditch along Drøbakveien in Ås, and materials that correspond to requirements from the Norwegian Public Roads Administration, will be used. In this part of the thesis, the fluorescent microplastic particles from part one will be utilised.

In order to answer to the research questions, an extensive literature study on microplastics, drainage systems and retention of microplastics in ditch materials, were conducted. Subsequently, experiments to stain particles from car tyres, and testing of ditch materials with particle suspension were conducted. Microscopy has also been a part of the process of analysing the results.

For part one of the thesis, it quickly became clear that black particles from car tyres were not possible to fluoresce. The results indicate that the dye itself attaches to the particles, but that it is still impossible to see them in the fluorescent microscope. This may be due to the colour or density of the particles. For part two of the thesis, it was possible to see high retention of microplastic in materials from both existing and constructed road ditches. This result is based on an estimate of both inlet and outlet concentrations from the ditch materials. Here, there may be some margin of error in the estimates, but essentially the results will be representative of realistic results.

Sammendrag

Denne avhandlingen omhandler mikroplast. Første del ser på muligheten til å bruke fluoriserende farging som en metode for identifisering og kvantifisering av mikroplast fra bildekk. Del to undersøker forskjellige grøftematerialers evne til å tilbake holde mikroplast. Her vil det bli sett på materialer fra den eksisterende veigrøften langs Drøbakveien i Ås, og materialer som samsvarer med krav fra Statens vegvesen. I denne delen av oppgaven vil de fluoriserende mikroplast partiklene fra del en bli benyttet.

For å svare på problemstillingene ble det først utført et omfattende litteraturstudie om blant annet mikroplast, drenerings system og tilbakeholdelse av mikroplast i grøftematerialer. Deretter ble det utført forsøk som gikk ut på farging av partikler fra bildekk og gjennomkjøring av partikkel suspensjon i grøftematerialer. Mikroskopi har også vært en stor del av prosessen for å bearbeide forsøkene.

For del én av avhandlingen ble det raskt klart at sorte partikler fra bildekk ikke var mulig å fluorisere. Resultatene indikerer at selve fargen fester seg til partiklene, men at det allikevel er umulig å se de i fluoriserende mikroskop. Dette kan være på grunn av partiklenes farge eller tetthet. For del to av avhandlingen var det mulig å se høy tilbakeholdelse av mikroplast i materialer fra både eksisterende og konstruert veggrøft. Dette resultatet er basert på et estimat av konsentrasjoner for både innløp og utløp fra grøftematerialene. Her vil det kunne være noen feilmarginer i estimatene, men i hovedsak vil tallene være representative for realistiske resultat.

Table of Contents

List of Figures

List of Tables

List of Acronyms

AADT	Annual average daily traffic
DLVO	Derjaguin-Landau-Verwey-Overbeek
FT-IR	Fourier transform infrared spectroscopy
GESAMP	Experts on the Scientific Aspects of Marine Environmental Protection
NIVA	Norwegian Institute for Water Research
NMBU	Norwegian University of Life Sciences
NPRA	Norwegian Public Roads Administration
PBR	Polybutadiene rubber
PC	Polycarbonate
PVC	Polyvinyl chloride
SBR	Styrene-butadiene rubber
TP	Tread particles
TWP	Tread wear particles
UNECE	United Nations Economic Commission for Europe
UNESCO	United Nations Educational, Scientific and Cultural Organization
WWTP	Waste water treatment plant

1. Introduction

In recent years, microplastic contamination of aquatic and terrestrial environments has received increasing attention (Lusher et al., 2018; GESAMP, 2016). A substantial number of studies have been published regarding microplastics in oceans, inland waters, and in waste water treatment systems, such as Enders et al. (2015), Thompson et al. (2004) and Eriksen et al. (2013). In 2013, the estimate of plastic in the oceans were 5.25 trillion particles, with a total weight of 268 940 tonnes (Eriksen et al., 2013). Recent studies suggest that a majority of microplastics in oceans originate from car tyres (Nerland et al., 2014). However, few countries have implemented solutions to capture the microplastic particles from road runoff, most end up freely in the environment (Vogelsang et al., 2018). Although some studies have been published about the emerging problem and its consequences, there is still a need for additional knowledge. Some scientists suggest that fluorescent staining can be utilised to identify and quantify microplastic particles from environmental samples (Erni-Cassola et al., 2017; Shim et al., 2016). However, the studies also report that fluorescent staining is ineffective on black plastic particles, such particles from car tyres. This could indicate that the estimated microplastic particles in aquatic and terrestrial environments are underestimated.

The objectives of this thesis are twofold: first, to examine the possibility of using fluorescent dye to stain microplastics, as a method for identification and quantification. Two dyes will be tested, Nile Red and Rhodamine B, together with rubber particles from recycled car tyres. The purpose of this would be to subsequently use the fluorescent particles for experiments on microplastic retention in the second part of the thesis. The second objective is to study the difference in removal of microplastics between an existing and a constructed road ditch. The experiment will be based on Drøbakveien in Ås municipality (Akershus) and requirements from Norwegian Public Roads Administration (NPRA) (Statens vegvesen, 2018b).

Based on this, the following research questions were developed:

- Can fluorescent staining with Nile Red and Rhodamine B be utilised as a method for identification and quantification of microplastic particles from car tyres?
- What is the retention capacity for microplastic particles in an existing road ditch compared to a road ditch that complies with current design guidelines?

1.1 Structure

This thesis consists of five chapters. The first chapter is this introduction. The second chapter is an extensive literature study into general microplastics, road drainage systems and microplastics in road runoff. Chapter three describes the methods and materials used in the experiments, whilst chapter four presents the results and the discussion of these, in addition to suggestions for further research. The last chapter presents a conclusion to the objectives.

2. Literature Study

This chapter presents relevant theory and background information that is essential to conceptualise the topic of this thesis. It is divided into three sections. Firstly, a section regarding microplastics, their occurrence, quantity and consequences in organisms and aquatic environments, and analytical techniques for sampling, identification and quantification, including fluorescent staining. Secondly, information about road drainage systems in Norway and specifically the drainage system for Drøbakveien. Lastly, microplastics from road runoff, its characteristics and occurrence and its retention in drainage systems.

2.1 About common microplastics

There are many different definitions of plastics, but they all share that they are solid materials that can be moulded, and consists of polymers. Usually it is only plastics that are mentioned as a problem and the source of microplastics. However, from an environmental point of view, both plastics and rubber are relevant as sources for microplastics, because both can produce solid particles with a high polymer content (Verschoor, 2015). Car tyres are usually a mix of styrene-butadiene rubber (SBR) and polybutadiene rubber (PBR), and a significant source of plastic particles (Vogelsang et al., 2018). Particles derived from tyres can be distinguished between pure tread particles (TP), which are typically carved out or shredded from car tyres and consists solely of rubber, and tread wear particles (TWP), which are generated by shear force and applied heat while driving and consists of a mix of both tread and road surface materials. TP make up approximately 40 % of TWP (Vogelsang et al., 2018). Most plastic and rubber types have low solubility as a common general characteristic, which means that components made of these materials will not dissolve and disappear, or dilute in aquatic environments (Verschoor, 2015). In 2013, the estimate of the total contents of plastic plastic in the oceans was 5.25 trillion particles, with a total weight of 268 940 tonnes (Eriksen et al., 2013). The majority of microplastic in both aquatic and terrestrial environments originate from car tyres (Nerland et al., 2014). In Norway, roughly 5000 tonnes end up on land, whilst 2500 tonnes end up in the seas. Other large sources of microplastics are paint, rubber granulates and wear and tear of textiles (Miljødirektoratet, 2019). An overview can be seen

in figure 2.1.

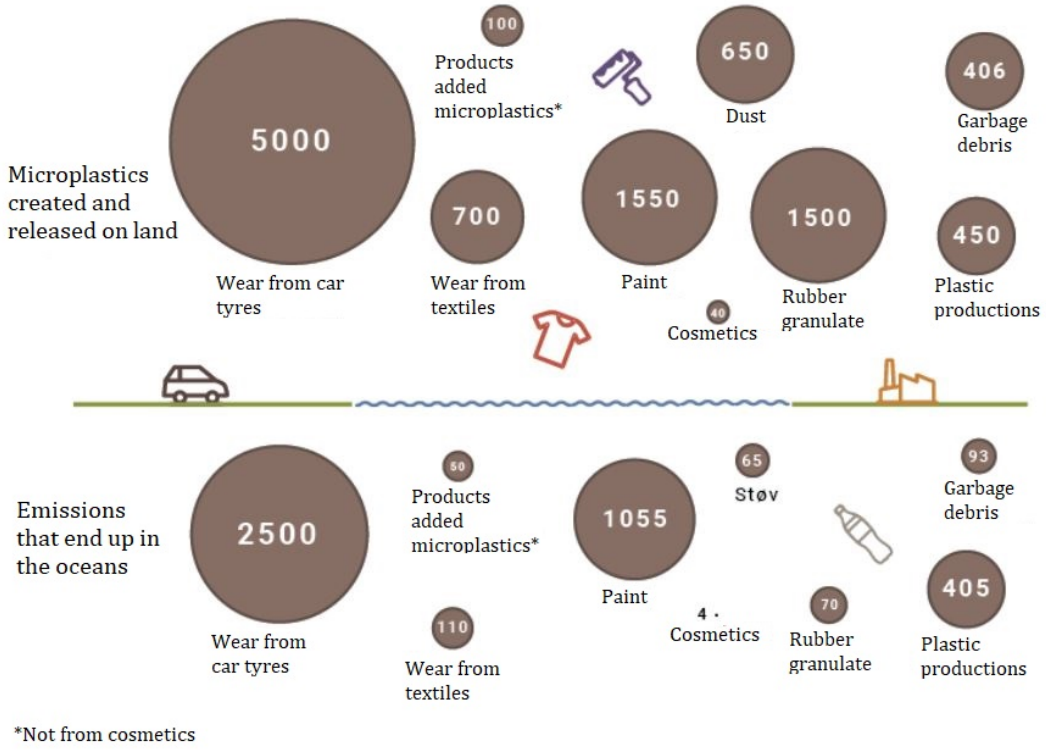

Figure 2.1: Sources of microplastics in terrestrial and aquatic environments (in tonnes per year). From Miljødirektoratet (2019).

Traditionally, microplastics have been defined as any plastic particle with a diameter less than 5 mm (GESAMP, 2016). A more precise definition of size range for plastic particles could refer to nano-, micro-, meso and macro-plastics, although this has yet to be formally proposed for adoption by the international research community (GESAMP, 2015). Vogelsang et al. (2018) adhered to the following size definitions in their report on microplastics in road dust:

- Macroplastics: > 25 mm
- Mesoplastics: 1-25 mm
- Microplastics*: 0.1-1000 μm
- Nanoplastics: < 0.1 μm

*The upper limit of the microplastic size were agreed upon by UNESCO at a meeting in September 2017(Vogelsang et al., 2018)

Microplastics can be divided into two groups; primary and secondary. Primary microplastics are manufactured to be small sized particles, often used in products such as cosmetics and body scrubs, production pellets and powders, and cleaning products. They are often released directly into the environment after use (Boucher and Friot, 2017). Secondary microplastics are particles caused by degradation and consequent fragmentation of larger plastic items, mostly due to weathering and mechanical tear (GESAMP, 2016). TP and TWP are in this category. Secondary microplastics are believed to be the main source of plastic particles in aquatic environments (Eerkes-Medrano et al., 2015).

2.1.1 Occurrence and quantity in organisms and aquatic environments

Several studies have concluded that marine animals ingest microplastics. A study conducted by Murray and Cowie (2011) found high concentrations of plastic particles in the decapod crustacean, Norwegian lobster (*Nephrops norvegicus*). 83 % had plastic particles in their stomachs, whilst 62 % had tangled balls of plastics strands. Lusher et al. (2013) found that out of ten fish species sampled from the English Channel, all ten had ingested microplastics, whilst Anastasopoulou et al. (2013) found evidence of plastic debris ingestion in 5 out of 24 species sampled from the Ionian Sea. Large amounts of plastic debris are also found on beaches and the sea floor. Samples from the Portuguese coast indicates that the number of particles found in sediments can be up to 2420 per m^2, whilst in Japan they found that 80-85 % of the debris on the sea floor was plastic (Nerland et al., 2014).

Eerkes-Medrano et al. (2015) write in their review that several freshwater field- and laboratory studies conclude that brackish fish, freshwater invertebrates, amphidromous fish and freshwater fish can ingest microplastics. One of these studies was a freshwater river field study conducted by Sanchez et al. (2014), who examined fish from eleven rivers in France. Seven of these rivers had Gudgeon (*Gobio gobio*) which contained microplastics, and 12 % of all the fish examined had ingested it. Plastic particles in freshwater does not only affect fish and invertebrates. Studies show that animals across habitats, feeding guilds and trophic levels ingest microplastics (Imhof et al., 2013), and that microplastics accumulate on lake beds. In a study conducted by Lusher et al. (2018) on behalf of The Norwegian Institute for Water Research (NIVA), sediments from 20 different sites in Lake Mjøsa were analysed for microplastics greater than 36 μm. Plastic particles were found in sediments from all sites. They also analysed ten sites within Lake Femunden, where eight sites showed evidence of microplastics particles.

Despite the increasing number of scientific studies on the occurrence, transport and distribution of microplastics in aquatic environments, and its effects on aquatic life, scientists have only recently begun to assess the potential effects on human health (Barboza et al., 2018). One of the first studies to estimate humans' potential exposure of microplastics through ingestion of seafood was conducted by Van Cauwenberghe and Janssen (2014). They concluded that in European countries with a high consumption of shellfish, the citizens will ingest up to 11 000 microplastic particles per year, whilst citizens in countries with low consumption of shellfish will ingest roughly 1800 microplastic particles per year. In recent times, several studies have shown that food and drinks consumed by humans, such as mineral water (Schymanski et al., 2018; Cox et al., 2019), beer (Liebezeit and Liebezeit, 2014), sea salt (Kosuth et al., 2018) and canned sardines (Karami et al., 2018), are contaminated with microplastics. Cox et al. (2019) estimated that microplastic consumption among Americans is in the range between 39 000 and 52 000 particles per year, depending on age and gender. When taking inhalation into account, the range is increased to 74 000 to 121 000 particles. In addition they explored whether the source of the drinking water could affect the consumption of microplastic particles. They found that a person who meet their recommended water intake through only bottled water may consume an additional 90 000 microplastic particles annually, compared to 4000 microplastic particles for those using only tap water (Cox et al., 2019). However, even though evidence shows the presence of microplastic in several food and drink items, there is insufficient research on the fate and consequences of microplastics in the human body after ingestion (Wright and Kelly, 2017; Barboza et al., 2018).

2.1.2 Consequences for organisms and aquatic environments

The knowledge about effects, accumulation and consequences of plastics in freshwater systems is less than for marine systems (Thompson et al., 2009; Wagner et al., 2014). This is concerning because humans are fully dependent on freshwater for drinking and for food resources. Eerkes-Medrano et al. (2015) published a review on microplastics in freshwater systems and its emerging threats. The review indicates that freshwater systems share several similarities to marine systems when it comes to, for example, the prevalence of plastic particles and the potential consequences they have for the aquatic environment. This could make it easier to tackle the arising issues surrounding microplastics in freshwater systems.

Microplastics can contribute to the spread of substances which are harmful to both the environment and human health, because the plastic itself contains these substances, but also because harmful substances can adhere to the surface of the particles (Miljødirektoratet, 2019). Marine debris, in particular microplastics, provides a pathway which facilitates the transport of chemicals to organisms. Chemical signals communicate many critical life processes, such as reproduction, feeding and benthic settling, for aquatic organisms (Webster and Weissburg, 2009). If these chemical signals are tampered with, it could have severe consequences for the organisms. In addition to toxicological effects, a laboratory study conducted by Wright et al. (2013a) indicates that microplastic ingestion might have physical effects on organisms and their food assimilation, such as decreased energy reserves in marine worms. Yet, physical impacts remain largely understudied (Wright et al., 2013b).

Sessile organisms may collect plastic particles, and provide a means of transportation for alien species in the aquatic environment, which may threaten the aquatic biodiversity (Moore, 2008). There is also a potential danger to the aquatic ecosystem from the accumulation of plastic debris on the sea- and lake floors. The debris can inhibit gas exchange between overlying water layers and the pore water in sediments, and in this way disrupt or destroy inhabitants of the benthos (Moore, 2008). For instance, laboratory experiments show that micro- (and macro) plastics significantly reduces skeletal growth rates for cold-water corals (Chapron et al., 2018).

TWP have been described as an aquatic toxicant, due to their potential for provoking endocrine disruption, teratogens and death (Wik and Dave, 2006; Gualtieri et al., 2005). Tyre wear and tear are presumed to cause local inflammatory effects in the intestinal lumen, in addition to potentially leaching toxic substances to the intestinal tissue (Jan Kole et al., 2017). Moreover, some studies have evaluated the potential of airborne tyre particles to provoke *in vitro* or *in vivo* pulmonary toxicity, suggesting that inhalation of TWP could entail negative health effects for humans (Gualtieri et al., 2005; Mantecca et al., 2005).

At the present time, there are no specific requirements in Norway for removing any kind of microplastics from water or waste water before discharging it into the receiving environment (Vogelsang et al., 2018). Most runoff from Norwegian roads ends up in aquatic environments without any treatment, except runoff from very polluted roads, which usually are treated in sedimentation ponds. Regardless, a substantial amount of microplastics from tyre wear and tear and road wear end up freely in the environment (Vogelsang et al., 2018). Research shows that the largest wastewater treatment plant (WWTP) in Norway, Vestfjorden

Avløpsselskap, receives over one billion microplastic particles every hour (Magnusson, 2014). Although most WWTPs are able to retain 87-97 % of the larger plastic particles, several million microplastic particles will be released into receiving aquatic environments every hour. The plastic particles which are being withheld, end up in the sewage sludge, which in Norway are largely used as a fertiliser for green areas and agricultural fields. Because of this, most microplastics will eventually end up in the environment even after treatment (Miljødirektoratet, 2019). However, because Norway is a part of the European Economic Area, and thus subjected to the Water Framework Directive, Norwegian authorities issued a corresponding regulation, the Norwegian Water Regulation, to ensure the national implementation of the directive (NIVA, 2017). With this implementation, the vulnerability of an aquatic recipient has to be taken into consideration before discharging treated water into the recipient. In addition, several research groups are examining and evaluating the toxicity of tyre debris in aquatic environments (Kreider et al., 2010).

These are just a few of the documented consequences of microplastics in aquatic environments and aquatic life, still it highlights its importance as a component of aquatic debris, and supports its recent identification as one of the top emerging global issues (Gall and Thompson, 2015).

2.1.3 Methods for sampling, identification and quantification

Despite an increasing amount of knowledge on the presence of microplastics in aquatic environments, the cost and arduousness of collecting the plastic particles limits the knowledge of temporal and spatial distributions; techniques are in general time consuming and unable to identify all particles (Eerkes-Medrano et al., 2015; Hidalgo-Ruz et al., 2012). The current methodology for quantification of microplastic in aquatic environments is inhibited by the lack of sufficiently sensitive methods (Erni-Cassola et al., 2017). The data generated from these methods can be underestimated due to human error in common methods. The need to develop faster, less expensive and more accurate methods has been clearly identified as a policy priority by the Marine Strategy Framework Directive (Hanke et al., 2013). This section will review a few of the most common methods used for sampling, identification and quantification of microplastics. This section will also elucidate the method of utilising fluorescent staining to identify and quantify microplastics.

According to Hidalgo-Ruz et al. (2012) there are three main sampling strategies in aquatic environments: selective, bulk, and volume-reduced. Selective sampling in the field is a

direct extraction of items that are easily recognised with the human eye, usually items on the surface of waters or sediments. This method is often applied to plastic pellets, because their size range makes them easy to detect. Bulk sampling is a method where an entire volume of samples is analysed without being reduced during the sampling. This method is usually used in situations where the items cannot be easily identified visually. Volume-reduced sampling in both sediment and water samples is when the volume of a bulk sample is reduced during the sampling. When using this method only the section of the sample that is of interest for further processing is kept (Hidalgo-Ruz et al., 2012). Both bulk and volume samples require further processing in a laboratory.

The most common method to identify microplastics is with infrared spectroscopy (Eerkes-Medrano et al., 2015). This method compares the infrared spectrum of a known polymer with the spectrum of an unknown plastic sample. The functional groups in a polymer absorbs the infrared energy, which leads to changes in the vibrations within the functional group. As a result, the specific functional groups can be identified, and used for comparison (Moody et al., 2004). There are different types of spectroscopy that can be applied to identify microplastics, such as Fourier transform infrared spectroscopy (FT-IR), infrared spectrophotometer and near-infrared spectrometer (Eerkes-Medrano et al., 2015). Another recognised method is Raman spectroscopy, which is used for of very small microplastics (<20 μm) (Araujo et al., 2018). It detects vibrations including a change in polarisability, and can compare it to the vibrations of a known substance. Raman spectrometers are divided into two categories: Fourier transform instruments and dispersive instruments (Le Pevelen, 2017). The method is far from predominant, because of disadvantages such as long measurement time, and proneness to spectral aberrations induced by fluorescence (Araujo et al., 2018).

After identifying the microplastics, the next step is usually quantification. A successful method of separation and quantification is the Munich Plastic Sediment Separator, developed by Imhof et al. (2012). The method applies a high-density separation fluid to separate plastic particles in a range of sizes. It works for all polymer types, different size classes and for particles with varied physical properties (Eerkes-Medrano et al., 2015).

A novel method for identifying and quantifying microplastic in aquatic environments is using fluorophores for luminescent staining. This type of study has been successfully conducted by Erni-Cassola et al. (2017) and Shim et al. (2016). Both plastics and fluorophores are hydrophobic. Therefore, if they are both added to an aquatic environment, they will aggregate and adhere to each other. In order to observe the luminescence of the fluorophore,

a fluorescent microscope have to be utilised. The illumination light from the microscope is absorbed by the fluorophore, which in turn emits a longer, low energy wavelength light. This light is separated from the surrounding light with filters designed for the specific wavelength, which allows the observer to see only the fluorescent light (Bradbury and Evennett, 1996). The principle of a fluorescent microscope can be seen in Figure 2.2. Samples with fluorescent particles can be added to a hemocytometer, a counting-chamber device used in microscopy, engraved with a laser-etched grid of perpendicular lines (Fuentes, 2019). The grid makes it possible to count the number of particles per square. After microscopy, image analysis software, such as ImageJ, can be utilised for automated particle recognition and quantification based on the fluorescent images. The method of using fluorophores to identify and quantify microplastic particles can also be implemented for environmental samples, as per Erni-Cassola et al. (2017) and Shim et al. (2016). However, both of these studies found that stained black plastic fluoresced poorly or not at all. This could indicate that microplastics from tyres often go undetected when using this method on environmental samples.

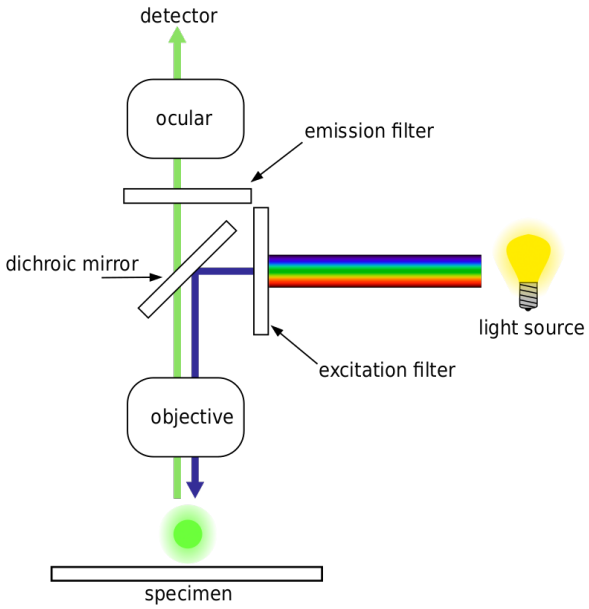

Figure 2.2: Principle of a fluorescent microscope. From Blachnicki (2006).

Two acknowledged fluorophores are Nile Red and Rhodamine B. These are the fluorophores tested in this thesis. Nile Red is a hydrophobic fluorophore and a histological dye. It binds specifically to neutral lipids, and is strongly luminescent in a hydrophobic environment (Greenspan et al., 1985). It is an organic heterotetracyclic compound, an aromatic amine, a cyclic ketone, and a tertiary amino compound, that is 5H-benzo[a]phenoxazin-5-one substituted at position 9 by a diethylamino group (National Center for Biotechnology Information, 2019a). The fluorescence intensity of Nile Red is affected by its concentration,

which is optimal between 0.1 and 2.0 μg/mL (Erni-Cassola et al., 2017), and according to Rumin et al. (2015) will lead to quenching at higher concentrations. The dye adsorbs onto surfaces of plastics, and renders them luminescent when irradiated with blue light (Maes et al., 2017). The fluorophore has a peak excitation and emission spectra at 515-530 and 525-605, respectively. Rhodamine B is a highly water soluble, basic red dye. It has a role as a fluorochrome, a fluorescent probe and a histological dye. It is widely used as a dye in textiles and food, and has also been used as a water tracer by Richardson et al. (2004). Ingestion is harmful to humans, and it can cause irritation to the eyes, skin and respiratory system through contact (Jain et al., 2007). It is an organic chloride salt and a xanthene dye having N-[9-(2-carboxyphenyl)-6-(diethylamino)-3H-xanthen-3-ylidene]-N-ethylethanaminium as the counterion (National Center for Biotechnology Information, 2019b). The fluorophore has a peak excitation and emission wavelength at 540 and 625, respectively.

2.2 Road drainage systems

Water entering the road structure poses an immense threat to the bearing capacity of the road. To ensure that water does not enter the road structure, it is necessary with effective and functional drainage systems. The NPRA distinguishes between open and closed drainage systems (Statens Vegvesen, 2014). An open drainage system is often a deep ditch on the side of the road that transports surface- and road runoff to a maintenance hole, whilst a closed system combines a shallow ditch and drainage- and transportation pipes. Recommendations for the choice of drainage system are based on annual average daily traffic (AADT) and speed limit (Statens vegvesen, 2018b).

In 2018, Drøbakveien in the municipality of Ås had an AADT of approximately 11500 (Statens vegvesen, 2018a), which according to the NPRA handbook *N200 Vegbygging* requires a closed drainage system to handle the road runoff (Statens vegvesen, 2018b). The purpose of a drainage system is to lead the runoff away from the road structure, so it is important that the materials used in the ditch are small enough to prevent infiltration. The handbook states that a closed drainage system should have sealants with d_{10}[†] $\leqslant$ 0.01 mm and C_u[‡] $\leqslant$ 20 (Statens vegvesen, 2018b). This gives a $d_{60} \leqslant 0.2$ mm, and categorises the materials as mostly coarse silt and fine sand (Statens vegvesen, 2010), as shown in Figure 2.3 (note that the graph is mirrored compared to Norwegian standard). However, according to Fredrik Nyland, Quality Control Engineer at

[†] d_n: n % of the mass consist of grains smaller than d_n
[‡] uniformity coefficient, $d_{60}/_{10}$ (unitless)

Oppland NPRA (telephone conversation, 4^{th} of April 2019), side ditches to older roads like Drøbakveien are usually built with available materials from nearby areas. This means that side ditches in Norway could consist of any range of material sizes.

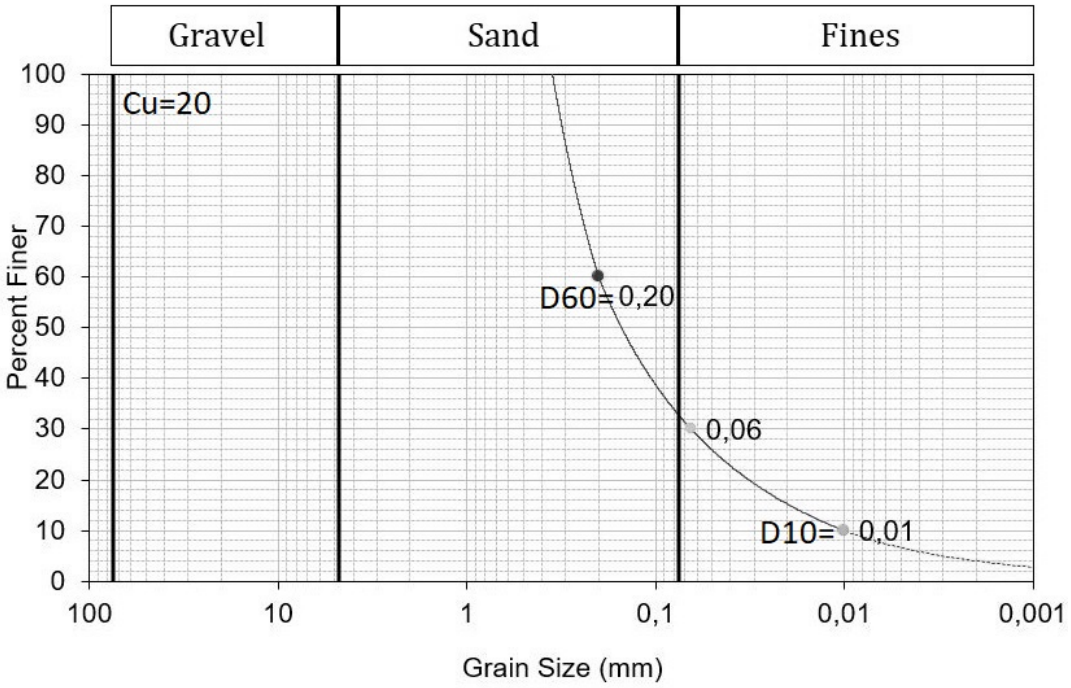

Figure 2.3: Estimated particle size distribution for a closed drainage system as required by the NPRA.

2.3 Microplastics in road runoff

Large amounts of microplastics are deposited along roads due to tyre wear and tear. The rubber may release chemical compounds that percolate to the ground water, and are toxic to some aquatic organisms (Wik and Dave, 2006). However, there is insufficient research on microplastics from tyre wear generated from driving and from road wear in Norway, and the effects it may have on the surrounding environment (Sundt et al., 2014; Kreider et al., 2010).

Due to the shear forces and the heat applied to the tyres when they abrade, TWP contain a mix of rubber and road materials (Vogelsang et al., 2018; Kreider et al., 2010). Moreover, rubber-containing particles in road dust are likely to be assimilated with materials from other traffic related sources, such as fuel and breaks (Adachi and Tainosho, 2004). Therefore, the characteristics of particles generated from actual driving are likely to vary from the original tyre tread particles, as well as from the particles generated from laboratory

rolling machines. Because of this, TWP will have a significantly higher density compared to standard microplastics. Reported densities for TWP are usually between 1.7 and 2.1 g/cm^3, but 2.53 g/cm^3 have also been reported (Snilsberg, 2008; Kayhanian et al., 2012), whilst standard microplastics have a density in the range of 0.9 to 1.5 g/cm^3 (Nerland et al., 2014). TWP are generally elongated with rough surfaces, which makes them similar to other typical road wear particles, although they are usually somewhat larger in size (Kreider et al., 2010). Lassen et al. (2015) claim TWP are predominantly coarse particles in the range 2.5 to 10 μm, whilst Kreider et al. (2010) claim the average size volume are between 65 to 85 μm. However, according to Vogelsang et al. (2018) there is insufficient data available to indicate the variability of particle size distribution for TWP.

The first annual estimate of TP emissions from tyre wear and tear in Norway were published in 1989 by Syversen (1989), and calculated to be approximately 6000 tonnes per year. In 2014, Sundt et al. (2014) used three different methods to update the estimate of the amount of microplastics from tyre wear and tear in Norway. First, by using annual running vehicle kilometres of passenger cars and heavy transport, and factors from United Nations Economic Commission for Europe (UNECE, 2013) for intensity of tyre wear, they calculated the accumulated tyre road dust to approximately 7520 tonnes per year. When assuming the rubber content in tyre road dust to be roughly 60 %, it amounts to approximately 4500 tonnes of rubber particles from tyres, i.e microplastics. Second, by using annual running vehicle kilometres of passenger cars and factors from Luhana et al. (2004) for intensity of tyre wear, they calculated the particles generated by tyre wear to be 3000 tonnes per year. In this part they do not include heavy transport, or comment on the amount of polymer particles in road dust. Third, they calculated the emission of microplastics based on tyre return to *Norsk Dekkretur*[§]. The total loss of mass from all tyres was 9571 tonnes in 2013. Assuming a 60 % share of synthetic material, the annual emissions of TP amounts to approximately 5700 tonnes. The latest estimate was conducted in 2018 by Vogelsang et al. (2018), based on annual travelled distance for all vehicles in Norway and a specific tread emission factor for these vehicles from Klein et al. (2017). They calculated the estimated annual emissions of TP to be 7080 tonnes, and microplastics due to tread wear on Norwegian roads to be 4250 tonnes per year.

These numbers highlight why several scientists suggest that wear and tear from car tyres is an important source of microplastics in the environment, and why it is critical to address it (Sundt et al., 2014; Jan Kole et al., 2017; Nerland et al., 2014).

[§]Norsk Dekkretur AS is a joint industry solution for collecting and recycling discarded tyres

2.3.1 Retention of microplastics in drainage systems

Several factors, such as water chemistry, particle properties, hydrodynamic conditions and soil/sediment properties, influences a particles potential mobility in natural aquatic environments (Wiesner and Bottero, 2007). Microplastics in natural soils and waters will be subjected to several processes that will affect their aggregation, deposition, and transport. These processes are largely dependent on aquatic chemistry, aquifer pore waters, and the properties of the sediment, and will directly affect the fate of the plastic particles in the environment (Alimi et al., 2018).

When particles collide with each other (aggregation) or with a collector grain surface (deposition), the probability of attachment is controlled by Van der Vaals and electrical double layer forces, as described by the Derjaguin-Landau-Verwey-Overbeek (DLVO) theory (Verwey et al., 1948), as well as non-DLVO-forces, such as steric forces (Alexander, 1977). The probability of attachment is referred to as *attachment efficiency* (α), and is the ratio between the collisions that result in attachment and the total number of collisions. If α approaches 1, the process is deemed diffusion limited and attractive forces influence the likelihood of attachment. If repulsive forces dominate, the process is deemed reaction-limited and α is less than 1 (Alimi et al., 2018). By reducing the repulsive forces one can achieve a higher rate of aggregation or deposition. According to DLVO-theory, this can be done by for example increasing the ionic strength of a solution (Verwey et al., 1948).

Several mechanisms can separate particles from water during filtration. If a particle is larger than the void spaces in the filter media, the removal is referred to as straining (Ødegard et al., 2014). In addition, if the diameter of a spherical particle is greater than 15 % of the diameter of the filter media, the particle will be strained by the filter media (Crittenden et al., 2012). If the particle is smaller than the voids, it can only be removed through definite contact with the filter media, where it adheres to the grains. This is called depth filtration (Crittenden et al., 2012). The particles will be continuously removed throughout the filter media by transport and attachment. The attachment can transpire by attractive distance-dependent interaction forces such as the van der Waals forces and electrostatic forces (Ødegard et al., 2014).

Various experiments have been conducted in order to study microplastics' deposition-kinetics in systems representative of the saturated and unsaturated zones in subsurface environments (Alimi et al., 2018; Masliyah, 1998). Most experiments use clean glass beads or high-purity quarts to represent soil or sediment. However, these materials poorly represent natural environments; research suggests that the behaviour of plastic particles are different in "dirty" conditions. Bouchard et al. (2012) found that the retention of polystyrene microplastics was greater in sediments from a small river in Georgia, USA, than in pure quartz sand.

As mentioned in section 2.2, the requirements for closed drainage systems are that 60 % of the masses are smaller than 0.2 mm. When implementing the principle explained above, it results in particles greater than 0.03 mm (30 μm) being retained by the ditch by straining. However, because the diameter of the remaining 40 % of the materials are unknown, but greater than 0.2 mm, microplastic particles smaller than 50 μm will most likely be retained.

When quantifying fluorescent particles, for example when utilising a hemocytometer, there is always a chance that the counter is unable to detect any particles. In these situations, it is possible to implement a detection limit for the instances where the count is zero. Detection limits are often used with viruses and bacteria, but can be altered to be suitable for fluorescent particles. To find the detection limit, the smallest concentration (C_L), which makes it unlikely (less than 5 % probability) that there are no particles in a hemocytometer square, must be determined (Friborg, 2015). This means that if no particles are observed in any of the hemocytometer squares, it can be said with 95 % certainty that the concentration in the sample is less than C_L. C_L can be calculated using the following equation, based on the Poisson distribution (Haas et al., 1999):

$$C_L = \frac{\ln 20}{\sum_{i=1}^{k} r_i V_i} \tag{2.1}$$

Where r_i is the dilution factor for hemocytometer square i, V_i is the volume of hemocytometer square i, and k is the number of hemocytometer squares.

3. Methods

This chapter will present the methods and materials used in the thesis. The chapter is divided into two parts. Part one will describe how Nile Red and Rhodamine B were assessed as fluorophores to stain tyre rubber, and the analytical work that follows. Part two will present the experiments used to assess the microplastic retention capacity of different roadside ditch materials, including the materials procured, the apparatus built to run the experiments and the actual runs that were conducted.

3.1 Part one: Fluorescent staining of microplastics

In an attempt to make fluorescent microplastic particles, three experiments were conducted. The first two tested both Nile Red and Rhodamine B, whilst the last tested only Nile Red. Rhodamine B were chosen as a cheaper alternative to Nile Red. Nile Red was purchased from Thermo Fisher Scientific as a 100 μg vial with dark red powder, and Rhodamine B were purchased from Alfa Aesar as a 250 g container with red powder. Both dyes were tested on black shredded rubber from recycled car tyres, donated from Ragn-Sells AS. The tyre rubber is mainly made up of styrene-butadiene rubber (SBR) and are available in three classes; fine (0–1.2 mm), medium (1–2.5 mm) and coarse (2.8–4 mm). The purpose of staining the black rubber is so that it can later be used in part two of this thesis, and in that way realistically represent the microplastic particles found in side ditches, whilst at the same time being easy to identify and quantify.

3.1.1 Attempt one of fluorescent staining

Nile Red is commonly dissolved in acetone, but based on the research of Erni-Cassola et al. (2017), it was decided to dissolve it in methanol, because common plastics are more resistant to it. A solution of 1.0 μg/ml was made for Nile Red, based on the methods of Erni-Cassola et al. (2017), whilst a solution of 2.5 μg/ml was made for Rhodamine B. In order to test the fluorescence of both Nile Red and Rhodamine B on different microplastic sizes, samples of fine, medium and coarse black rubber particles were prepared. The different sizes were placed

on individual glass microfiber filter (Whatman 47-mm Ø, 1.2 μm pore size) and soaked by dripping approximately 3 ml of Nile Red and Rhodamine B respectively, rinsed well with distilled water, then stored in the dark for a few days to ensure they were properly dried before microscopy.

Microscopic imaging was performed using a Leica DMRE fluorescence microscope. The samples of microplastics were tested with both green (em: 500-550 nm, ex: 450-490 nm) and red (em: LP 590 nm, ex: 515-561 nm) fluorescence. During the microscopy it became evident that the dye had not adhered to the entire surface of the particles, but instead had only stained the surface in small, isolated areas. It was therefore necessary to conduct further tests.

3.1.2 Attempt two of fluorescent staining

In an attempt to increase the adhesion between the dyes and the rubber, a second experiment was conducted, with the concentration of Nile Red and Rhodamine B increased to 5 μg/ml and 50 μg/ml, respectively. For Nile Red, 5 μg/ml was chosen based on the finding of Shim et al. (2016) for optimal concentration. In addition, it was decided to submerge the samples in 1 ml of the dyes to ensure total coverage of the entire surface, as opposed to dripping the dye on the samples. In an attempt to reduce background staining on the filters, two new filter types were also tested. The filters were cellulose nitrate membrane filters (Schleicher and Schuell 47-mm Ø, 0.45 μm pore size) and cellulose filter paper (Aoshi 47-mm Ø, 8.0 μm pore size). During the preparation for the filtration, it became apparent that the pore size of the cellulose nitrate membrane filter was so small that the filter was practically impervious, thus it was decided to discard it from the experiment. The last modification made to the experiment was to limit the rubber samples to particles smaller than 50 μm, based on the notion that particles bigger than this will be withheld at the surface of a side ditch, as mentioned in section 2.3.1. After all the modifications were made, the same procedure as in the first attempt was followed: the submerged particles were added to the filters and rinsed well with distilled water to limit the background staining on the filters, then kept in the dark for a few days before microscopy.

Microscopic imaging of the samples from the second experiment was conducted with a Leica DM6 B fluorescence stereo zoom microscope. As in the previous attempt the particles, as well as the two filter types, were examined with green (em: 500-550 nm, ex: 450-490 nm) and red (em: LP 590 nm, ex: 515-561 nm) fluorescence. When examining the samples dyed with Rhodamine B, a drop of oil was added to the sample on the microscope slide, in order

to increase the resolving power of the microscope. It was once more evident that the dyes had not stained the microplastic particles. It was also apparent that the cellulose filter paper absorbed both dyes, whilst the glass microfiber filter did not absorb any dye whatsoever. On this basis, it was decided to exclude cellulose filter paper from further experiments.

3.1.3 Attempt three of fluorescent staining

In the final attempt to make the black rubber particles fluoresce, it was decided to test only Nile Red and discard Rhodamine B. In addition it was decided to dissolve Nile Red in acetone, because that is the standard for Nile Red solutions. The Nile Red powder was dissolved 0.1 % in acetone (prepared by Hilde Raanaas Kolstad at NMBU Imaging Centre). Tyre particles smaller than 50 μm were submerged in the solution for one hour, then filtered through glass microfiber filter, as mentioned in section 3.1.2. Subsequently the sample was kept at 60°C for 10 minutes in the dark, as described by Erni-Cassola et al. (2017). This sample of dyed microplastics was not rinsed with water during the filtration.

Microscopic imaging of the sample for the third experiment was conducted with a Zeiss Axio Zoom.V16 fluorescence microscope. In view of the fact that red fluorescence has been inferior to the green fluorescense in previous examinations, it was decided to utilise only green fluorescense with em: 500-550 nm and ex: 450-490 nm. However, the plastic particles did still not fluoresce.

3.2 Part two: Retention of microplastics in drainage systems

After part one of the experimental work was completed, it was clear that it was not possible to make the procured black rubber tyre fluoresce. It was therefore decided to purchase microspheres that were already fluorescent. The intent was to purchase three different sizes, 30, 10 and 1 μm in order to examine a wide range of sizes, but it became apparent that microspheres are excessively costly, therefore it was decided to only utilise 1 μm microspheres. Due to the fact that it is not possible to find microspheres with properties identical to the black rubber, part two of this thesis will be an approximation to actual conditions. The microspheres were purchased from BaseLine ChromTech Research Centre, and were green fluorescent and made of polystyrene with a density of 1.05 g/cm^3.

In order to study the difference in retention rate between an existing and a constructed side ditch, materials from both were acquired. Materials in the range 0 - 2 mm were donated by Franzefoss Pukk AS, to construct a filter medium as similar as possible to the requirements from the Norwegian Road Association (NPRA) for a side ditch. To get results as representative as possible, it was decided to obtain material samples from three different locations in the side ditch next to Drøbakveien in Ås, and to extract three samples from each location. An overview of the locations can be seen in Figure 3.1. In an attempt to preserve the layer structure and the density of the soil as much as possible, cylinders of soil cores were extracted from the ditch by using a soil auger, then carefully transferred to Polyvinyl chloride (PVC) columns for further experiments. In addition to the three samples, an additional sample for particle size distribution analysis was collected from each of the three locations.

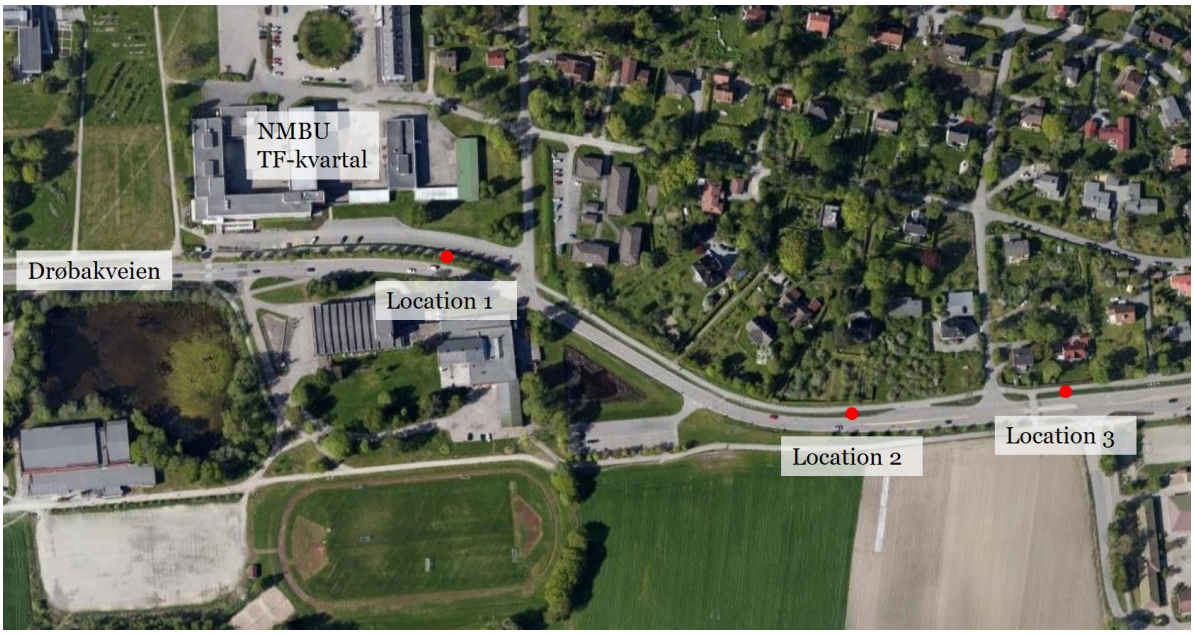

Figure 3.1: Overview of the locations for sampling of soil from a side ditch. Background map from Google Maps.

3.2.1 Particle size distributions

To determine the particle size distribution of the materials, a wet sieve analysis was conducted with 20 grams of the materials. The mesh widths of the sieves were 2 mm, 600 μm, 212 μm, 63 μm and 20μm. This means that the materials larger than the mesh width were withheld in the respective sieve, and that the materials smaller than 20 μm were transported with the water to the drain. The materials from each sieve were transferred to beakers and left in a heating chamber overnight at 105 °C so that the water in the beakers evaporated and only the sample materials were left. After the samples were completely dried, each beaker was weighed to determine the weight of each fraction, which subsequently was used to create a graph for grain size distribution. The calculations for these graphs can be seen in Appendix A.

The particle size distribution graphs for the three ditch samples can be seen in figures 3.2, 3.3 and 3.4. From the graphs it is apparent that the materials for sample 1 and 2 are mostly sand, and that the materials from sample 3 are mostly fines. This illustrates why it is important to sample different locations in the ditch; the local differences can be quite significant. Figure 3.5 shows the materials received from Franzefoss Pukk, which ideally should be identical to the graph shown in Figure 2.3. However, they are not. Because of this,

it was decided to conduct a new sieving with roughly 5 kilograms of the materials, and to reconstruct the size composition to coincide with requirements from the NPRA, as mentioned in section 2.2. This material will be referred to as *materials according to the NPRA* in this thesis, and 4.1, 4.2 and 4.3 in the calculations. Because of limitations to the sieving process, it was not possible to separate the masses to fractions smaller than 20 μm or larger than 212 μm. The graph for the new particle size distribution can be seen in Figure 3.6, whilst the calculations can be seen in Appendix A. Three columns with this material (4.1, 4.2 and 4.3), in addition to the nine samples taken from the ditch, are being tested in this experiment.

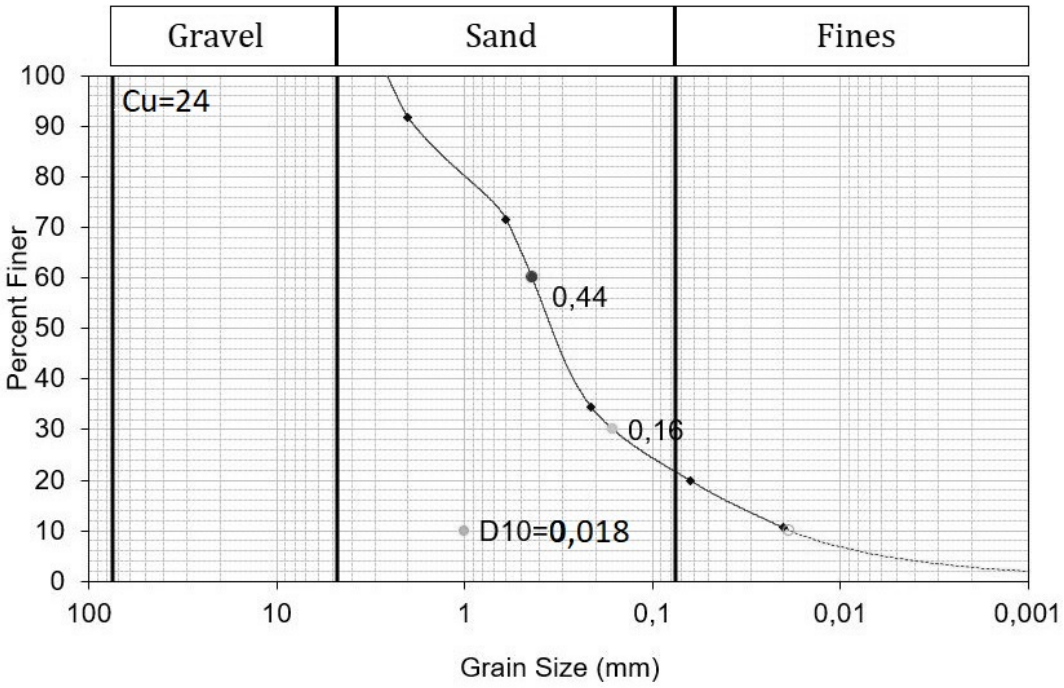

Figure 3.2: Particle size distribution from location 1.

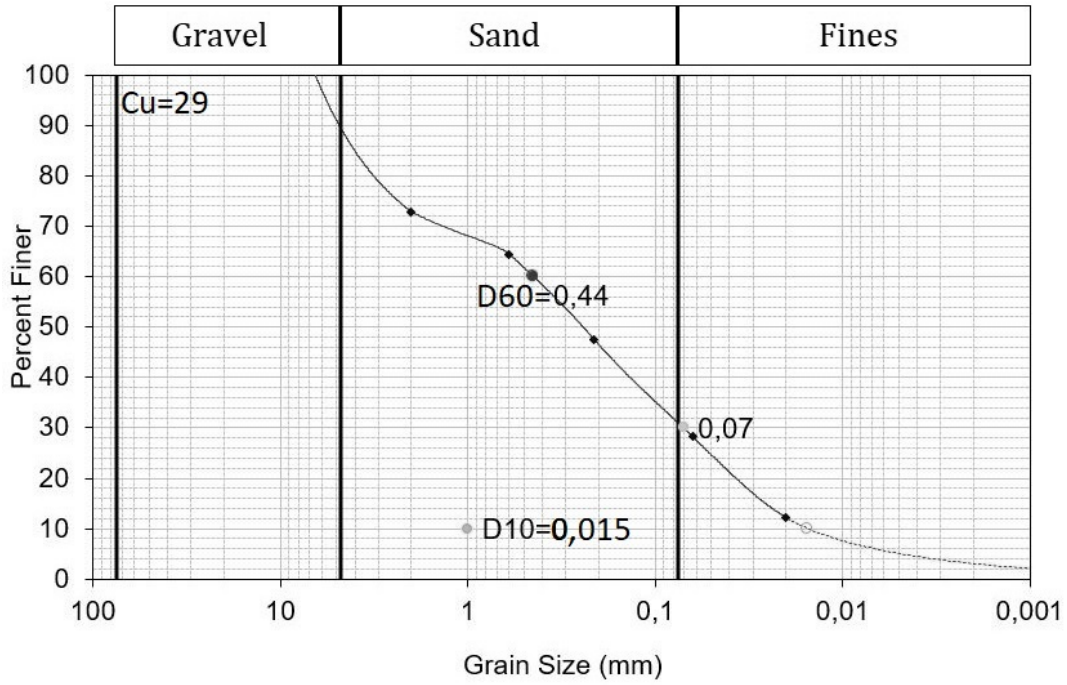

Figure 3.3: Particle size distribution from location 2.

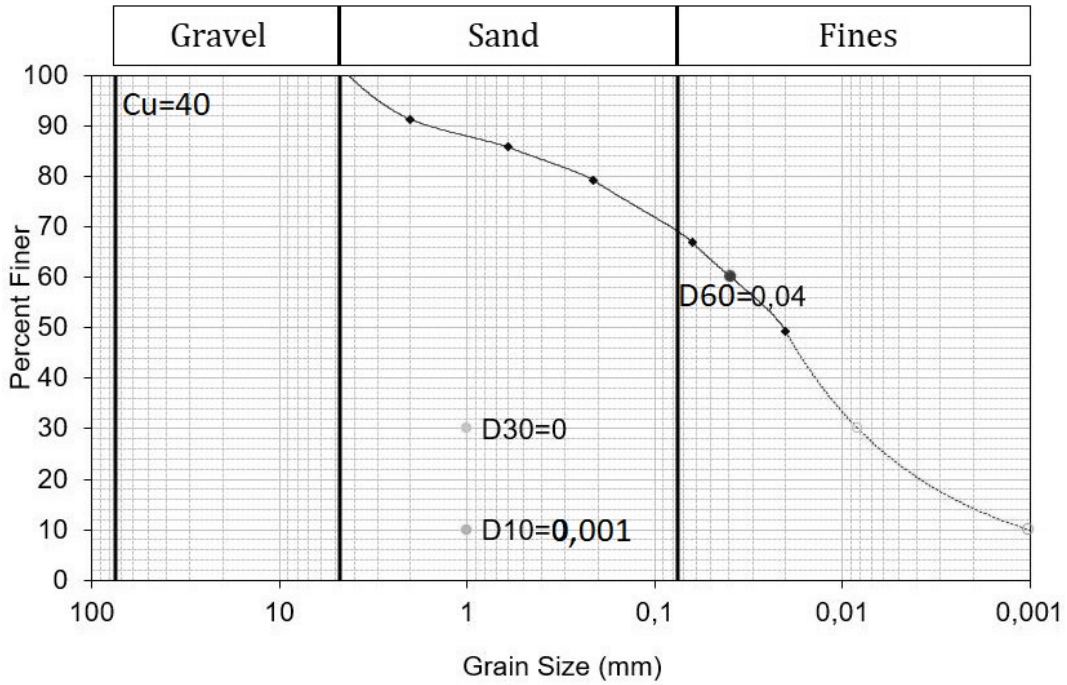

Figure 3.4: Particle size distribution from location 3.

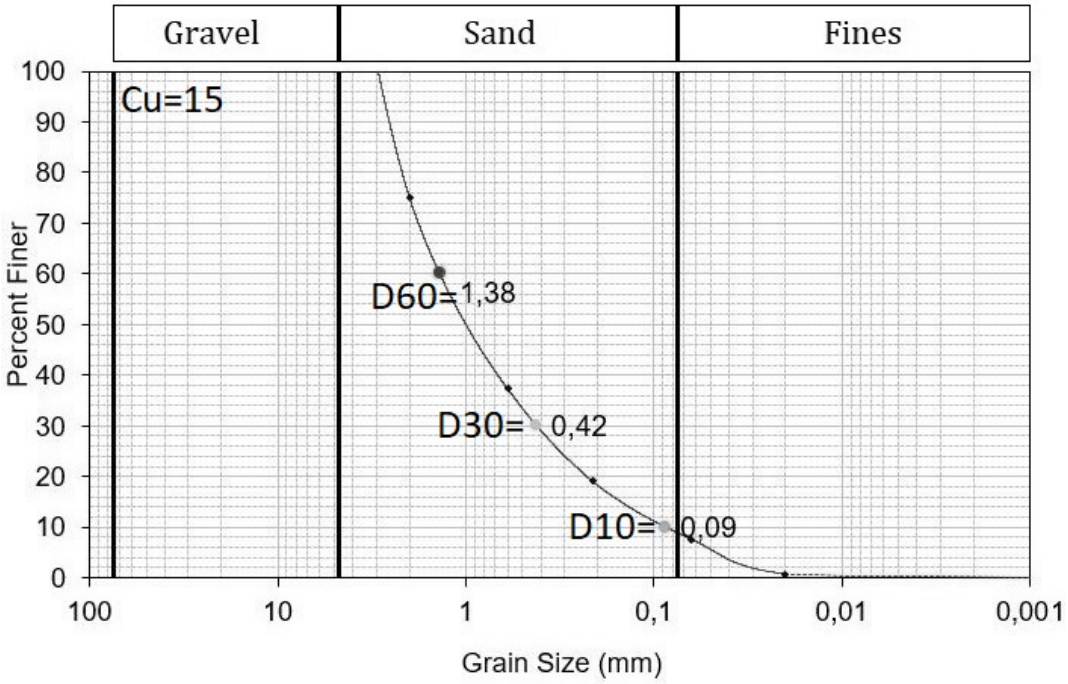

Figure 3.5: Particle size distribution for the materials donated by Franzefoss Pukk.

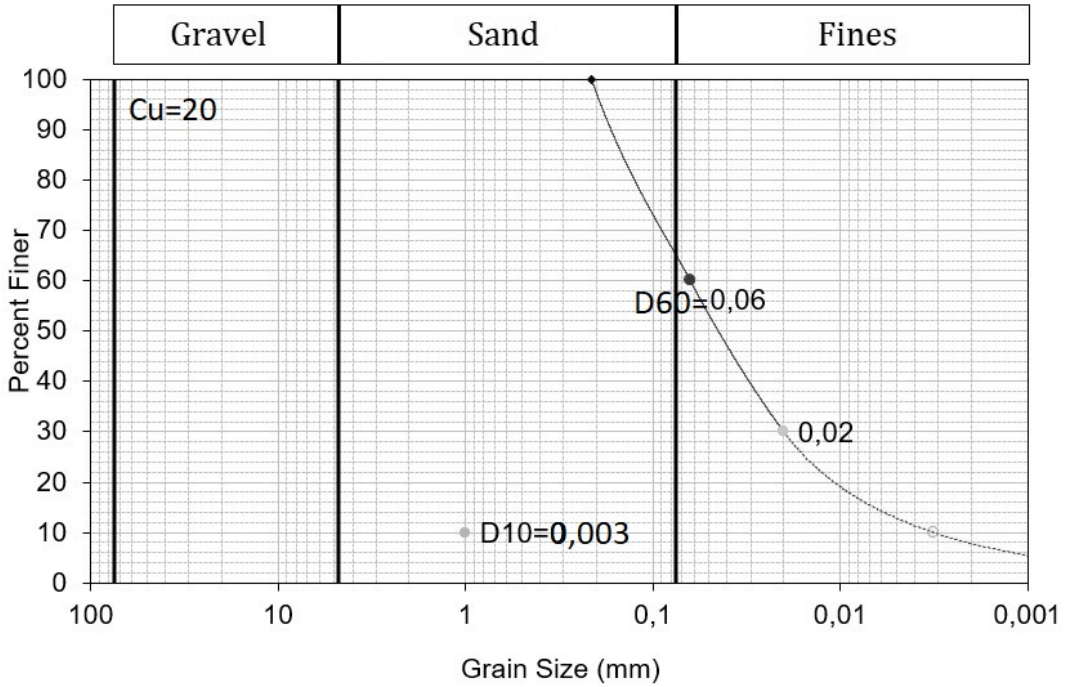

Figure 3.6: Particle size distribution for the materials according to the NPRA.

3.2.2 The experimental apparatus

The apparatus was built to operate six columns with filter media at a time, which means it had to be run twice to test all twelve columns. It is operated with a multichannel peristaltic pump, that transports an equal amount of water to each column. The six columns are fastened next to each other on a wooden plank that is mounted to the wall. At the bottom of the columns there are silicone tubes attached, that lead the filtered water to an overflow chamber to keep the outlet hydraulic head fixed. This ensures a stable hydraulic gradient in each column when the pump gives off a steady volumetric flow. The overflowing water is then led to a bucket for disposal. A photograph of the apparatus can be seen in Figure 3.7.

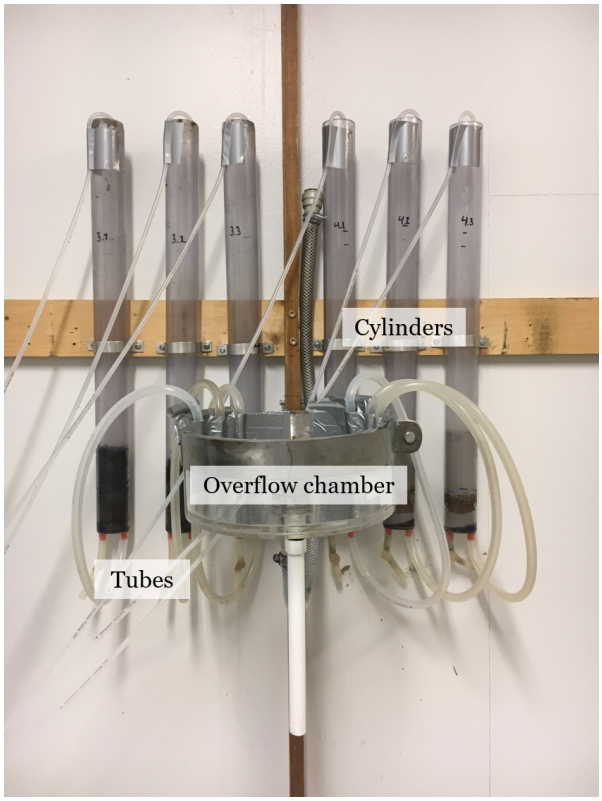

Figure 3.7: The experimental apparatus.

3.2.3 Test runs for hydraulic stabilisation

For the purpose of stabilising the water levels in the columns so that they are prepared for the main runs, and so that it later would be possible to calculate the entire necessary volume for the main runs, a test run of all the columns were conducted with tap water. By calculating the average precipitation for Ås based on data from eKlima (2018), it was decided to use a precipitation rate of 0.14 mm/min. However, this would only be for the actual ditch. In a realistic situation, the ditch would also receive runoff from the road and pavement. Based on the assumption that a column will receive ten times the precipitation, a column will receive 1.4 mm/min. With a column diameter of 3.8 cm, this gives a volumetric flow rate of 1.6 ml/min, which the pump was set to.

During the stabilisation run for the filter media from location 3 and the materials according to the NPRA, it became apparent that the water levels in the columns were high over the filter media. This could indicate that the hydraulic conductivity in these materials are very low. The overflow was lowered 16 cm in order to lower the water level in the columns, and the system was left to stabilise with these conditions. After a while the water level in the columns with filter media from location 3 stabilised, however the water level in the columns with materials according to the NPRA were still rising. Upon closer inspection it became apparent that the sand in the filter media was so fine, that it was transported with the water flow from the columns to the overflow, and clogged the tubes (Figure 3.8). The tubes were drained, and it was decided to try to place a filter between the columns and the tubes, in order to detain the filter media in the columns. Both glass microfiber filters and cellulose nitrate filters were tested, both tore when subjected to water. Coffee filters were also tested, and they did not tear. However, this did not solve the problem, it only moved the clogging to the columns instead. Another solution tested, was to make a column of the coffee filter and placing it in a new, empty column, and subsequently transferring the filter media to the new column. Nevertheless, this attempt was also futile. In the end, the solution was to make a small sieve of metal, with pore size roughly 20 μm, that was placed in the bottom of new, clean columns. The original columns with the filter media according to the NPRA were drained and placed in a heating chamber to dry. In this way the filter media was kept intact, and could later be transferred to the new columns.

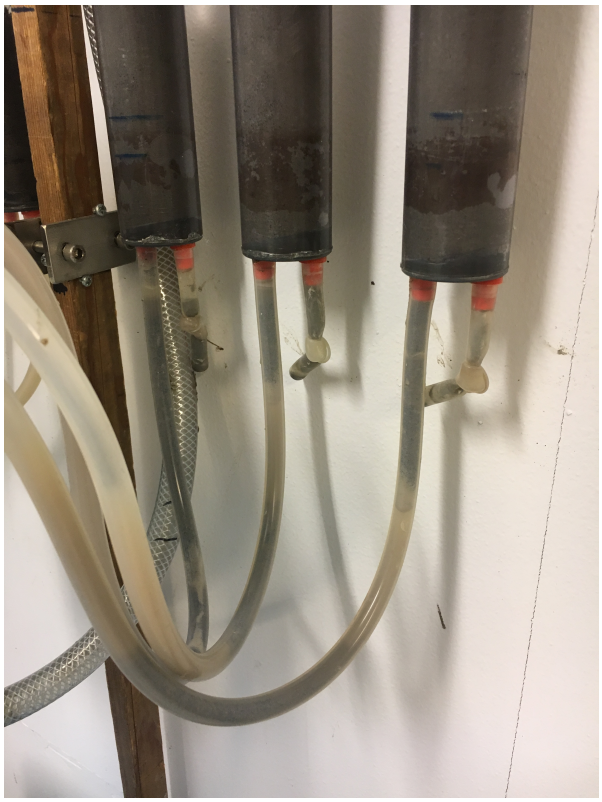

Figure 3.8: Clogged tubes in the second stabilisation run.

After a new stabilisation run of the filter media from location 3 and the materials according to the NPRA, it became clear that the hydraulic conjunctivitis in the different filter media were very variable. The water levels in columns 3.1, 4.1, 4.2 and 4.3 were very high, whilst the water levels in columns 3.2 and 3.3 were much lower. It was therefore decided to divide these columns into two separate main runs.

After the system stabilised for the various test runs, the depth of the filter media (L) and the hydraulic head (ΔH) for each column were measured, in addition to the water volume above the filter media and the water volume in the tubes. These measurements and several calculations, such as volume per filter, hydraulic conductivity (k) and hydraulic head gradient (i), were performed in order to calculate a total water volume for the entire system (as mentioned previously). To ensure that the full volume of tap water remaining in the system after the test run was replaced with stormwater during the actual experiments, and to obtain a stable particle removal, it was decided to utilise three times the necessary volume. The measurements and calculations can be seen in tables 3.1, 3.2 and 3.3.

Table 3.1: Calculations for the first main run.

Parameter	Method	1.1	1.2	1.3	2.1	2.2	2.3
Q [ml/min]	From pump	1,600	1,600	1,600	1,600	1,600	1,600
Q [m3/s]	Recalculated	2,667E-08	2,667E-08	2,667E-08	2,667E-08	2,667E-08	2,667E-08
q [m/s]	Q/A	2,360E-05	2,360E-05	2,360E-05	2,360E-05	2,360E-05	2,360E-05
q [ml/min]	Recalculated	1,416	1,416	1,416	1,416	1,416	1,416
L [m]	Measured	0,107	0,070	0,143	0,066	0,076	0,073
ΔH (m]	Measured	0,019	0,019	0,057	0,033	0,004	0,042
i	ΔH/L	0,178	0,271	0,399	0,500	0,053	0,575
k [m/s]	q/i	1,329E-04	8,694E-05	5,920E-05	4,720E-05	4,484E-04	4,102E-05
n	From table*	0,400	0,400	0,400	0,400	0,400	0,400
v [m/s]	q/n	5,900E-05	5,900E-05	5,900E-05	5,900E-05	5,900E-05	5,900E-05
t [sek]	L/v	1813,65	1186,50	2423,85	1118,70	1288,20	1237,35
V [m3]	Q·t	4,836E-05	3,164E-05	6,464E-05	2,983E-05	3,435E-05	3,300E-05
V filter [l]	Recalculated	4,836E-02	3,164E-02	6,464E-02	2,983E-02	3,435E-02	3,300E-02
V extra [l]	Measured	0,05024	0,08424	0,04692	0,09958	0,06065	0,10250

VOLUMES	
Sum. vol. filter[l]	0,242
Sum. vol. extra[l]	0,444
Tot. Vol. · 3 [l]	2,058

Table 3.2: Calculations for the second main run.

Parameter	Method	3.2	3.3
Q [ml/min]	From pump	0,667	0,667
Q [m3/s]	Recalculated	1,112E-08	1,112E-08
q [m/s]	Q/A	9,838E-06	9,838E-06
q [ml/min]	Recalculated	0,590	0,590
L [m]	Measured	0,081	0,076
ΔH (m]	Measured	0,104	0,286
i	ΔH/L	1,284	3,763
k [m/s]	q/i	7,662E-06	2,614E-06
n	From table*	0,400	0,400
v [m/s]	q/n	2,459E-05	2,459E-05
t [sek]	L/v	3293,43	3090,13
V [m3]	Q·t	3,661E-05	3,435E-05
V filter [l]	Recalculated	3,661E-02	3,435E-02
V extra [l]	Measured	0,080847900	0,077427300

VOLUMES	
Sum. vol. filter[l]	0,071
Sum. vol. extra[l]	0,158
Tot. Vol. · 3 [l]	**0,688**

Table 3.3: Calculations for the third main run.

Parameter	Method	3.1	4.1	4.2	4.3
Q [ml/min]	From pump	0,667	0,667	0,667	0,667
Q [m3/s]	Recalculated	1,112E-08	1,112E-08	1,112E-08	1,112E-08
q [m/s]	Q/A	9,838E-06	9,838E-06	9,838E-06	9,838E-06
q [ml/min]	Recalculated	0,590	0,590	0,590	0,590
L [m]	Measured	0,096	0,130	0,126	0,083
ΔH (m]	Measured	0,514	0,514	0,500	0,513
i	ΔH/L	5,354	3,954	3,968	6,181
k [m/s]	q/i	1,837E-06	2,488E-06	2,479E-06	1,592E-06
n	From table*	0,400	0,400	0,400	0,400
v [m/s]	q/n	2,459E-05	2,459E-05	2,459E-05	2,459E-05
t [sek]	L/v	3903,33	5285,76	5123,12	3374,75
V [m3]	Q·t	4,339E-05	5,876E-05	5,695E-05	3,752E-05
V filter [l]	Recalculated	4,339E-02	5,876E-02	5,695E-02	3,752E-02
V extra [l]	Measured	0,235555850	0,054380650	0,240320800	0,225668850

VOLUMES	
Sum. vol. filter[l]	0,153
Sum. vol. extra[l]	0,520
Tot. Vol. · 3 [l]	**2,021**

* Porosity from *Introduksjon til Geoteknikk (*Emdal, A*)*.

3.2.4 Main runs

The first main run was conducted with filter media from location 1 and 2, the second with two of the filter media from location 3, and the third with the last filter media from location 3 and the materials according to the NPRA. The runs were conducted with a particle suspension consisting of stormwater mixed with the fluorescent microspheres. The stormwater was collected from a stormwater pipe in Gamle Hogstvetvei, and consisted of runoff from both roads and rooftops, and waste water from households. Because the microspheres are so small, they adhere to each other. In order to properly disperse the particles in the stormwater, a ultrasonic bath were utilised. For run one, two and three the concentrations were 7.61 * 10^6, 4.41 * 10^6 and 4.93 * 10^6 particles/ml, respectively (calculations in Appendix B). After the system had stabilised, the tap water was substituted with the particle suspension and left to run long enough to properly replace all the tap water in the system (as mentioned in section 3.2.3). In order to get one sample per column that represents the particle removal at stable conditions, the tubes going from the columns to the overflow system were clamped shut in each end. By doing this it was possible to get enough volume in the samples, whilst at the same time leaving the system undisturbed. If the system was disturbed, by for example drawing water from the overflow into the tubes, it could result in the samples being altered, and thus useless. The samples from the tubes were transferred to beakers, and maintained in a dark refrigerator before microscopy.

Microscopic imaging was conducted with a Leica DM6 B fluorescent microscope. A drop of sample was added to a hemocytometer, and examined with a green fluorescence filter (ex: 470nm, em: 535nm) and a phase-contrast filter. The combination of these filters makes it possible to view the fluorescent particles and the grid in the hemocytometer at the same time. Because some of the samples contained both fluorescent particles and particles from the stormwater and/or the filter media, and because the identification of fluorescent particles is based on images taken during microscopy, it was decided to focus the microscope on the fluorescent particles to make them easier to identify from the images at a later time.

The hemocytometer has two grids made up of 144 squares (12 by 12) each. In order to estimate the number of fluorescent particles of each sample as accurately as possible, the fluorescent particles of 10 squares were counted for each grid, totalling in 20 squares per sample. These 20 squares were chosen at random. The average fluorescent particles per square was then calculated and divided by the volume a square in the hemocytometer contains, in this case 0.004 μl. The first attempt at counting the particles per square was conducted with ImageJ, to minimise human error. The colour threshold in the software was modified to coincide with the green fluorescence in the particles, then the area of the squares from the hemocytometer were selected, and lastly the program ran the particle recognition and quantification. However, after finding the initial concentration for the stormwater ($C_0$1, $C_0$2, $C_0$3) using this method, it was evident that the software overestimated the number of particles per square. The first calculation found that the total particles used were 5.687 * 10^{11}, but for this project only 1.7 * 10^{10} fluorescent particles were purchased. The use of recognition and quantification software was therefore discontinued, and it was decided to count the fluorescent particles manually. When doing this, it was decided to ignore some of the large clusters of particles, because it is impossible to both accurately count the number of particles in a cluster and to know if the particles are fluorescent particles or particles from the filter media.

In order to obtain some characteristics about the stormwater, tests for turbidity, conductivity and pH were conducted. The stormwater has a turbidity of 4.6 NTU. This could affect the removal of particles because the fluorescent particles might adhere to the particles in the stormwater. In addition, the particles in the stormwater could fill the pores in the filter media and thus alter the filtration capacity. The stormwater had a pH of 7.17. According to Li et al. (2018) (Supplementary Data Fig.S1) this gives a zeta potential of roughly -17, which means that the surface charge of the fluorescent microspheres is negative. The conductivity was 1115 mS/m, which is is quite high. For comparison, the limit for drinking water is 250 mS/m at 20°C (Helse- og omsorgsdepartementet, 2017).

3.2.5 Utilised equations

In order to conduct the experiments in this thesis, some simple equations have been utilised:

$$Q = A * q \tag{3.1}$$

$$q = i * k \tag{3.2}$$

$$i = \frac{\Delta H}{L} \tag{3.3}$$

$$v = \frac{q}{n} \tag{3.4}$$

$$t = \frac{L}{v} \tag{3.5}$$

$$V = Q * t \tag{3.6}$$

Where:

Q = Volumetric flow rate [m^3/s]
A = Cross area of cylinder [m]
q = Darcy velocity [m/s]
i = Hydraulic head gradient
k = Hydraulic conductivity [m/s]
ΔH = Hydraulic head [m]
L = Length of filter media [m]
v = Filter velocity [m/s]
n = Filter media porosity
t = Infiltration time in filter media [s]
V = Volume of water in filter media [m^3]

4. Results and discussion

This chapter will present the results of the experiments described in Chapter 3 and the discussion of these results, and is in the same way divided into two sections. Section one will present the results from microscopic imaging of fluorescent microplastic particles, whilst section two will present the comparison of retention of fluorescent microspheres in existing and constructed side ditch materials.

4.1 Part one: Fluorescent staining of microplastics

4.1.1 Attempt one of fluorescent staining

The aspect of this attempt that concerns Nile Red was conducted on the basis of Erni-Cassola et al. (2017), which indicates that the results should be similar. The microplastic samples were examined with a fluorescent microscope, with both green and red fluorescence. Green fluorescence was well recognised without significant background luminescence on the glass microfiber filter, for both Nile Red and Rhodamine B. red fluorescence could also be detected, yet it was less bright than green fluorescence, and the intensity of the background luminescence made the contrast between particles and filter low. For Nile Red these finding corresponds with the findings of both Shim et al. (2016) and Erni-Cassola et al. (2017). It was evident that neither Nile Red nor Rhodamine B had adhered to the entire surface of the black rubber particles, but instead had only stained the surface in small, isolated areas (Figure 4.1). This contradicts the findings of Erni-Cassola et al. (2017), who claim that black rubber (from bicycle tyres) did not fluoresce what so ever. With the particles only stained in patches, it is impossible to accurately quantify the particles, because one single particle could have more than one patch of dye, and thus look like multiple particles in a fluorescent microscope. There was no difference in fluorescence for the dissimilar sizes of microplastics, except that it was easier to see the patches of luminescent dye on the largest particles.

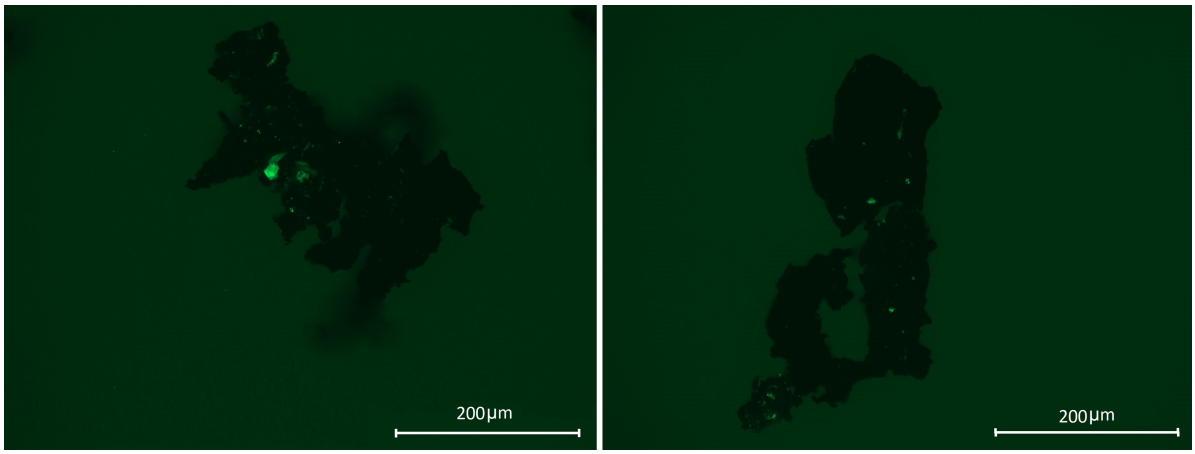

Figure 4.1: Photo of microplastic particles stained with Nile Red under a fluorescence microscope with ex: 450-490 nm and em: 500-550 nm.

4.1.2 Attempt two of fluorescent staining

The samples from the second experiment were also examined with both green and red fluorescence. As in the previous attempt, green fluorescence was deemed superior to red, therefore it was decided to exclude red fluorescence from further attempts. During the microscopy it was apparent that the cellulose filter paper absorbed both Nile Red and Rhodamine B, thus giving off a substantial amount of background luminescence. However, the glass microfiber filter was completely without fluorescence, and therefore deemed as the optimal filter to proceed with. Erni-Cassola et al. (2017) write in their article that they use black polycarbonate (PC) filter because its hydrophilic surface prevents background fluorescence. However, PC filters are quite expensive, so glass microfiber filters could be used as a cheaper option. From the microscopic images it was evident that the particles were not fluorescent, regardless of which dye was utilised. However, an interesting observation for this attempt was that for both Nile Red and Rhodamine B, other substances in the samples did fluoresce. When looking at the sample dyed with Nile Red, it was evident that the microplastic particles had unknown substances attached to it that had become fluorescent (Figure 4.2a). The substances were almost transparent and seemed to be less dense than the black rubber. For the sample dyed with Rhodamine B, the added drop of oil became luminous under the fluorescent microscope, even though it was added a week after the initial fluoresce attempt (Figure 4.2b). Both these findings can suggest that the fluorescent dye does adhere to the microplastic particles, but for some reason does not become luminous under a fluorescent microscope. One possible reason could be that the black rubber is too dense, thus not giving off any fluorescence. This is supported by Erni-Cassola et al. (2017), who found that polymers with higher density ($\geqslant$1.2 g/cm^3) fluoresced weaker than polymers with lower density

(<1.08 g/cm^3). In addition, Shim et al. (2016) found that black-coloured polyvinyl-chloride particles only fluoresced as a dim green glow. This could indicate that the colour of the microplastic is a potential reason as to why the samples did not fluoresce.

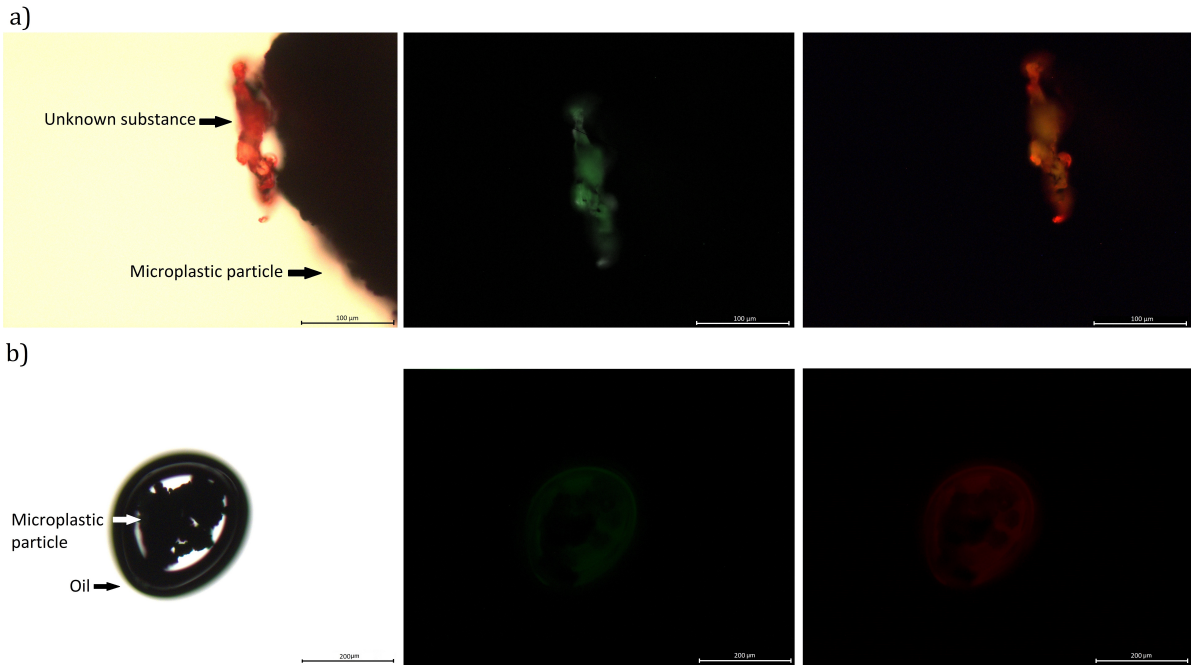

Figure 4.2: Photo under a regular microscope (left) and under a fluorescence microscope with ex: 450-490 nm and em: 500-550 nm (middle), and ex: 515-561 nm and em: LP 590 nm (right) of a microplastic particles stained with (a) Nile Red and (b) Rhodamine B.

4.1.3 Attempt three of fluorescent staining

As mentioned in section 3.1.3, the samples from the third experiment was tested with only Nile Red. As opposed to the previous attempts it was diluted with acetone, not methanol. Even though common plastics are less resilient to acetone, the black rubber particles did not seem to have been degraded by the acetone. The images from the microscopy became quite dark when adding the scale bars, but it was still possible to see that some areas of the microplastic particles had been stained with the dye (Figure 4.3). However, similar to the results of attempt one described in section 4.1.1, no particles' entire surface was fully fluorescent. The microplastic particles were only stained in small, isolated areas.

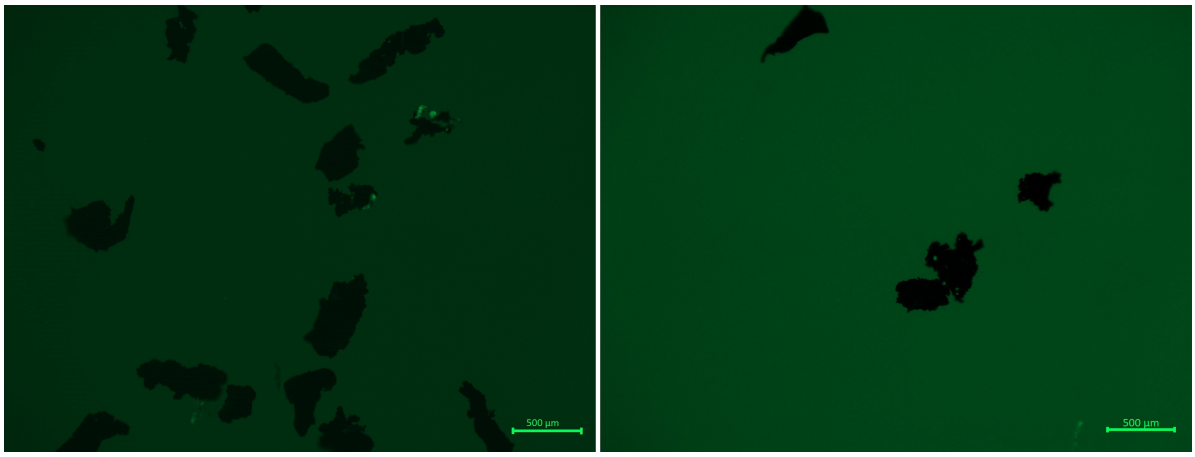

Figure 4.3: Photo of microplastic particles stained with Nile Red under under a fluorescence microscope with ex: 450-490 nm and em: 500-550 nm.

4.1.4 Reflections on fluorescing

After the three attempts, it was clear that the black rubber particles were impossible to fully fluoresce. According to Lene Hermansen, head engineer at NMBU Imaging Centre, it is possible that the fluorescent molecules do not bind to the plastic, or that it only partially binds to it (E-mail, 3^{rd} of May 2019). However, seeing as the particles fluoresced in small areas, and that the dye transferred to an added drop of oil, this seems likely that the dye does adhere to the plastic. Gabriel Erni-Cassola (PhD candidate, Warwick University, UK), lead author of Erni-Cassola et al. (2017), suggested that the samples are a type of composite that have other polymer bits in it, and that these polymer bits are fluorescing (E-mail, 8^{th} of May 2019). This seems like a reasonable explanation, considering the fact that in the first and third attempt the plastic fluoresced in isolated areas. A third reason could be the density and colour of the microplastic particles, as mentioned above. Nevertheless, at this time it is not possible to say with certainty why the black rubber particles do not fluoresce. It could however, mean that the estimated amount of microplastics in the environment are, or will be, underestimated, when fluorophores are applied as a method of identifying and quantifying microplastics.

4.2 Part two: Retention of microplastics in drainage systems

This section presents the results of the experiment conducted for part two of the thesis. The retention of fluorescent particles in materials from an existing and a constructed road ditch will be presented. In addition, the correlations of log-reduction and filter depth, filter coefficients and hydraulic conductivity, and uniformity coefficient and hydraulic conductivity will be presented. During the microscopy it became clear that sample 3.1 was so full of particles that the grid in the hemocytometer were impossible to see (Figure 4.4d). Thus, this sample were excluded from further consideration. The remaining eleven outlet samples, in addition to three inlet samples (C_0.1, C_0.2, C_0.3), were counted and analysed. The full results and calculations can be seen in Appendix B, whilst a summary can be seen in Table 4.1.

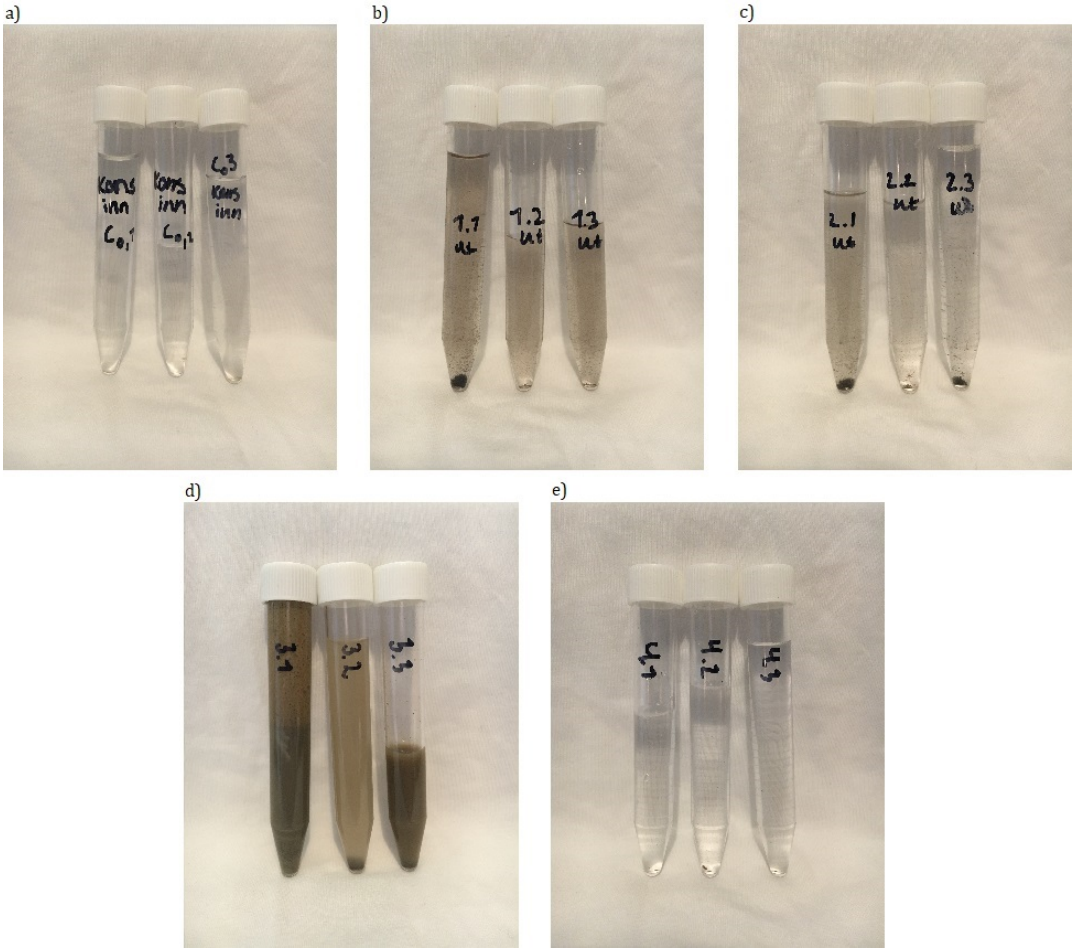

Figure 4.4: The samples used in part two of the experiment. A is the inlet samples. B, c and d are samples from the existing ditch. E is from the constructed ditch.

Table 4.1: The number of average particles per square and the estimated particle concentration for each sample.

	C_0.1	1.1	1.2	1.3	2.1	2.2	2.3
Average per square:	30.45	0.3	0.9	0,000	0.7	0.75	0.95
Total particles out:	-	2,57E+07	7,72E+07	12828200	6,00E+07	6,43E+07	8,15E+07
Total particles in:	1,57E+10	2,61E+09	2,61E+09	2,61E+09	2,61E+09	2,61E+09	2,61E+09
	C_0.2	3.2	3.3	C_0.3	4.1	4.2	4.3
Average per square:	17.65	0.7	0.15	19.85	0,000	0,000	0,000
Total particles out:	-	6,02E+07	1,29E+07	-	18896350	18896350	18896350
Total particles in:	3,04E+09	1,52E+09	1,52E+09	1,00E+10	2,51E+09	2,51E+09	2,51E+09

4.2.1 Comparison of particle reduction in existing and constructed ditch

Figure 4.5 illustrates the percentage reduction of fluorescent particles for each sample. It is clear that all the filter medias retained a lot of particles, all over 95 %. The three samples that represents a side ditch according to the NPRA (4.1, 4.2, 4.3) have a reduction of 100 % each. The usual representation of particle removal is by log-reduction, but because some of the sample had 100 % removal, it is impossible to accurately illustrate this as log-reduction. However, this can be rectified by implementing a detection limit (as mentioned in section 2.3.1). For this experiment, the detection limit will be as follows:

$$C_L = \frac{\ln 20}{20 * 0.0004\ \mu l} \approx 37400 \text{ particles/ml} \tag{4.1}$$

Figure 4.6 illustrates the log-reduction for each sample, when the detection limit is utilised. What this means, is that for sample 1.3, 4.1, 4.2 and 4.3 the reduction can be no less than log 2.309, 2.123, 2.123 and 2.123, respectively. The purpose of a side ditch is not to infiltrate the runoff, but to lead it away from the road structure (Statens vegvesen, 2018b). With more than 2.123 log-reduction for the NPRA samples, it indicates that this filter media is quite impermeable, thus fulfilling its purpose. The samples from the existing ditch also have quite high reduction rates, even one with 100 % reduction. In average the samples had reductions of 98.69 %, 97.37 % and 97.59 %, for location 1, 2 and 3, respectively. This could mean that the existing side ditch is built adequately and that it does not infiltrate the runoff.

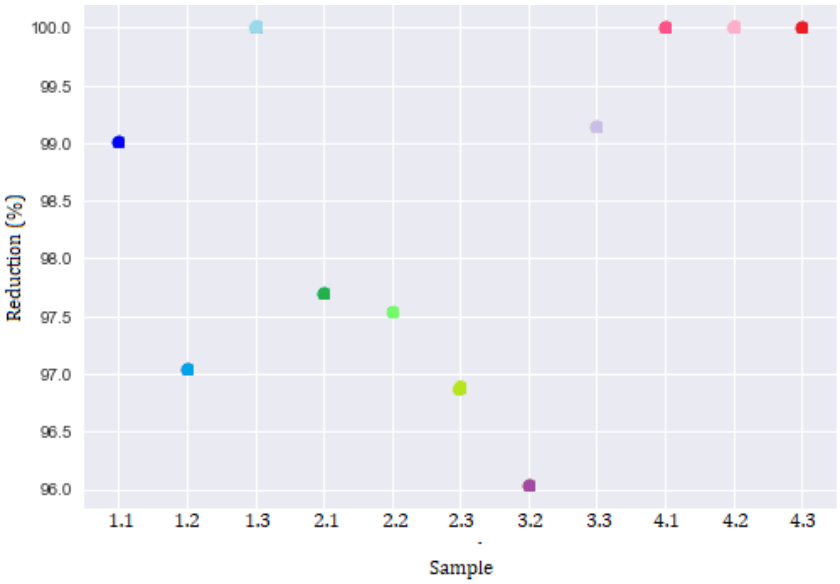

Figure 4.5: Percentage reduction of fluorescent particles for each sample.

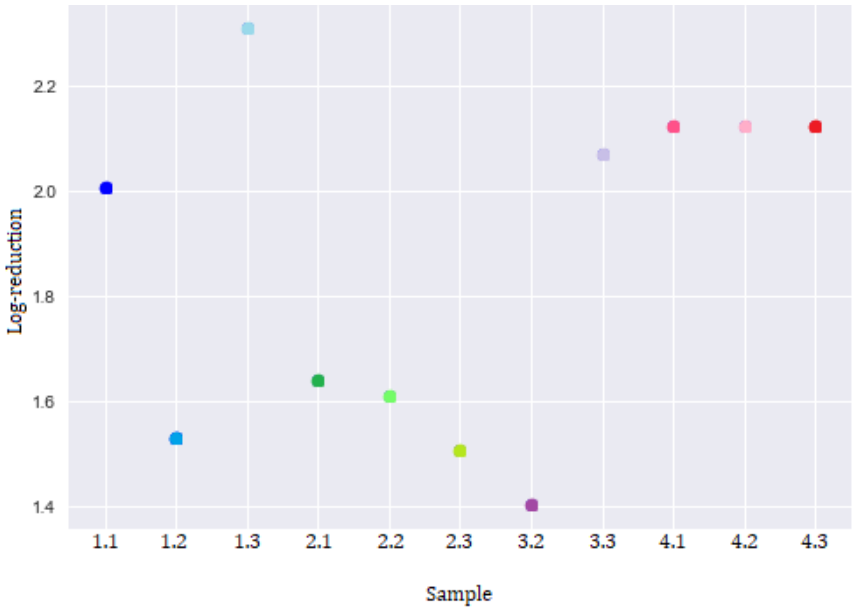

Figure 4.6: Log reduction of fluorescent particles for each sample.

Filter coefficients

When implementing the detection limit, it is also possible to calculate the filter coefficients for each sample. From Figure 4.7 it is apparent that many of the samples have filter coefficients that are quite similar (between 40 and 60 m^{-}1). However, some of the filter coefficients are higher, such as for sample 1.3, 4.1, 4.2 and 4.3. This coincides with the reductions illustrated in figures 4.5 and 4.6, and shows that the filter coefficient is directly dependent on the inlet- and outlet concentrations. However, it is also dependent on the depth of the filter media. This can be seen by the filter depths shown in Table B.3, where the filter depth of 4.3 is shallower than 4.1 and 4.2. Even though they have the same particle reduction, the filter coefficient for sample 4.1 is higher, because the filter depth is shorter. In these three samples the materials are equal, so this could be because of the filter medias density. This could indicate that with higher densities, a side ditch does not have to be so deep. Another interesting aspect to study is the relationship between the filter coefficients and the Darcy velocity for the corresponding filter media. This experiment in this thesis utilised two different Darcy velocities, which is expected to affect the filter coefficients. However, this requires additional filtration theory which is not included in this thesis. The calculations for the filter depths can be seen in Appendix B.

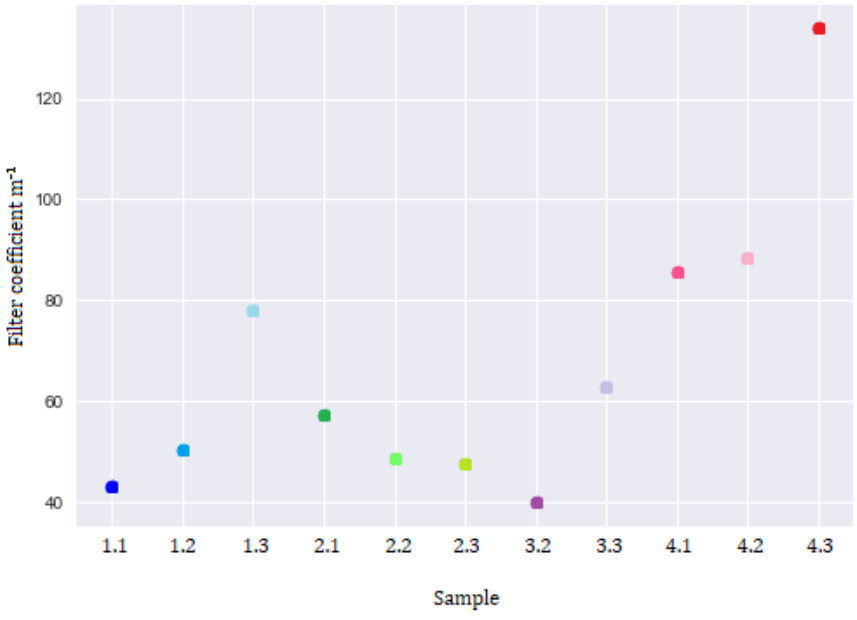

Figure 4.7: Filter coefficients for each sample.

4.2.2 Correlation of log reduction and depth of filter media

For the samples taken from the same location in the existing ditch, it would be reasonable to expect the filter media to have the same depth. However, as presented in tables 3.1, 3.2 and 3.3, the filter depth (L) from the same location can differ. Figure 4.8 shows the correlation of log-reduction and the depth of the filter media. For the most part, it looks like there is a correlation between the filter media depth and the reduction of fluorescent particles. The calculated correlation coefficient r is 0.7569. This is a moderate positive correlation, which means there is a tendency for high X variables to go with high Y variables. The calculations of the correlation can be seen in Figure C.1.

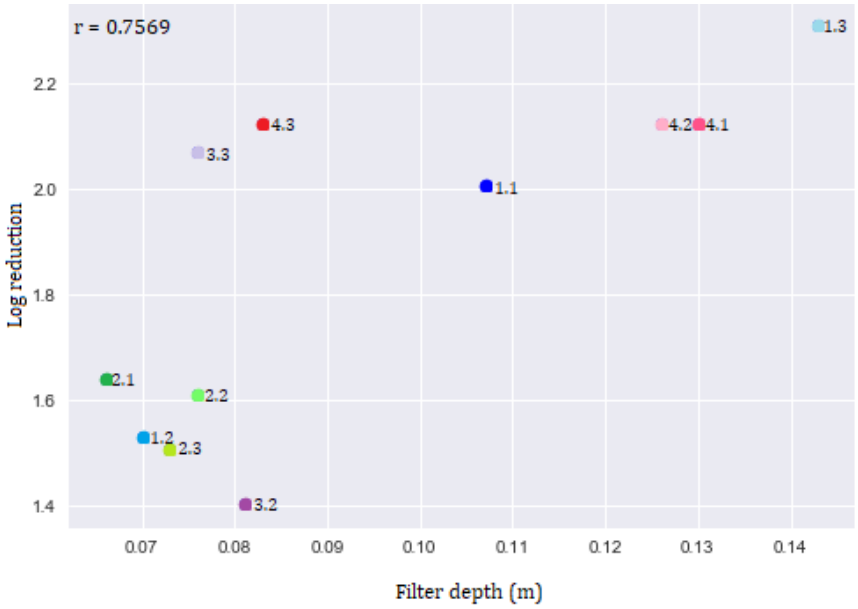

Figure 4.8: Correlation of log reduction and filter depth.

4.2.3 Correlation of filter coefficients and hydraulic conductivity

Figure 4.9 illustrates the correlation between filter coefficients and hydraulic conductivity. From the figure it is evident that there is no particular connection between the filter coefficients and the hydraulic conductivity. However, the figure illustrates well that the samples from the same location have similar hydraulic conductivity. The exception is samples from location 2, which in turn have similar filter coefficients, contrary to the other samples. The calculated correlation coefficient r is -0.3641. This is a a weak (negative) linear relationship between the reduction and the hydraulic conductivity. The calculations of the correlation can be seen in Figure C.2.

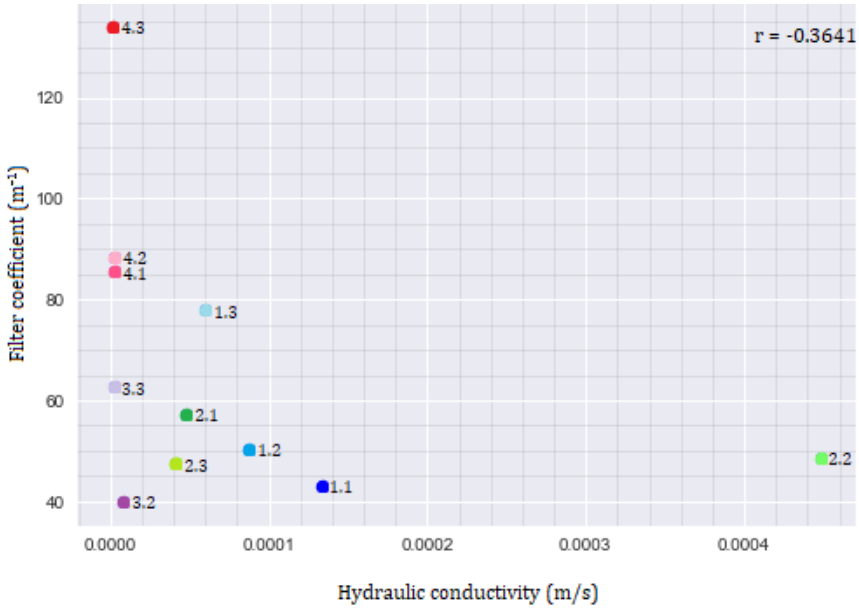

Figure 4.9: Correlation of filter coefficients and hydraulic conductivity.

5. Conclusions

The purpose of this thesis was twofold: First, to examine the possibility of using fluorescent staining as a method for identification and quantification of microplastic particles from car tyres. Second, to study the difference in retention capacity for microplastics between an existing and a constructed road ditch that complies with guidelines from the Norwegian Public Road Association.

The literature study revealed that several scientists have used fluorophores, in particular Nile Red and Rhodamine B, to stain microplastics from environmental samples. This has been an effective method for identification and quantification of plastic particles. However, some of these studies found that dark and dense microplastic particles were not so easy to fluoresce. That is also consistent with the findings of this study. After three attempts of staining black rubber from recycled car tyres, it became clear that fluorescing black rubber with Nile Red and Rhodamine B is futile. It is a known fact that car tyres is the largest source of microplastics in the environment, both aquatic and terrestrial. This could mean that large quantities of microplastics go undetected when utilising fluorophores for identification and quantification. When underestimating the amount of microplastic particles in the environment, the consequences for both humans and animals could also be underestimated.

The NPRA have strict requirements for how a drainage system should be built. However, most road side ditches in Norway are built with materials from nearby areas. This thesis studied the retention of fluorescent microspheres in materials from three locations in the side ditch to Drøbakveien, and in materials according to NPRA regulations. The results showed that the reduction of microplastic particles was more than 1.4 log-removal, for all materials. The initial quantification showed that all the samples with materials from the NPRA had an estimated removal rate of 100 %, and calculations showed that they had quite low hydraulic conductivity compared to most of the other samples. This indicates that these materials are working the way they are meant– to be an impervious surface next to the roads and lead the runoff away from the road structure. The materials from the side ditch of Drøbakveien had varying results in several aspects, such as retention, particle size distribution and hydraulic conductivity. Despite this they all had more than 96 % removal, sample 1.3 even had an

estimated removal of 100 %. This shows that the retention rate between an existing road ditch and a road ditch according to NPRA requirements are quite similar. Due to uncertainties with the estimated inlet and outlet concentration, it is impossible to find the exact retention rate. However, even if the estimate is wrong to some degree, the result would still be that both an existing and a constructed road ditch retain a great deal of microplastics, and will be representative of realistic results.

5.1 Further research

In regards of the black rubber particles that did not fluoresce, Gabriel Erni-Cassola (E-mail, 8^{th} of May 2019) suggested to scan some of the fluorescent spots with Micro Raman spectroscopy and see if those have different spectra from the black, non-fluorescent parts. In this way it is possible to examine if the particles consist of different polymer bits, and if these are the spots that are fluorescing.

For part two of this thesis, there are some aspects of the experiment that could be interesting to investigate further. Firstly, with the methods that have been utilised in this thesis, it is not possible to know how much of the fluorescent particles that were kept on the surface of the filter medias and how much that were deposited in the filter media. By examining this aspect further, it could be possible to know how much microplastics that are washed away with the surface runoff to either WWTPs or into aquatic environments, and how much that go into terrestrial environments. By having a more accurate estimate of the amount of microplastics in these environments, it could contribute to a further understanding of its consequences. Secondly, to study the difference in retention rate with saturated and unsaturated flow. The experiment in this thesis was conducted with a saturated flow, however, the flow of road runoff in side ditches are likely to be unsaturated. Lastly, how the use of nearby materials in road side ditches affect the infiltration of road runoff, and subsequently the bearing capacity of the road structure, as opposed to materials required by the NPRA.

References

Adachi, K. and Tainosho, Y. (2004). Characterization of heavy metal particles embedded in tire dust. *Environment International* 30 (8): 1009–1017. DOI: 10.1016/j.envint.2004.04.004.

Alexander, S. (1977). Adsorption of chain molecules with a polar head a scaling description. *Journal de Physique* 38 (8): 983–987. DOI: 10.1051/jphys:01977003808098300.

Alimi, O. S., Farner Budarz, J., Hernandez, L. M., and Tufenkji, N. (2018). Microplastics and Nanoplastics in Aquatic Environments: Aggregation, Deposition, and Enhanced Contaminant Transport. *Environmental Science and Technology* 52 (4): 1704–1724. DOI: 10.1021/acs.est.7b05559.

Anastasopoulou, A., Mytilineou, C., Smith, C. J., and Papadopoulou, K. N. (2013). Plastic debris ingested by deep-water fish of the Ionian Sea (Eastern Mediterranean). *Deep-Sea Research Part I: Oceanographic Research Papers* 74: 11–13. DOI: 10.1016/j.dsr.2012.12.008.

Araujo, C. F., Nolasco, M. M., Ribeiro, A. M., and Ribeiro-Claro, P. J. (2018). Identification of microplastics using Raman spectroscopy: Latest developments and future prospects. *Water Research* 142: 426–440. DOI: 10.1016/j.watres.2018.05.060.

Barboza, L. G. A., Dick Vethaak, A., Lavorante, B. R., Lundebye, A. K., and Guilhermino, L. (2018). Marine microplastic debris: An emerging issue for food security, food safety and human health. *Marine Pollution Bulletin* 133 (May): 336–348. DOI: 10.1016/j.marpolbul.2018.05.047.

Blachnicki, K. (2006). *Fluorescence Filters*. URL: https://commons.wikimedia.org/wiki/File:FluorescenceFilters.svg.

Bouchard, D., Zhang, W., and Chang, X. (2012). A rapid screening technique for estimating nanoparticle transport in porous media. *Water research* 47. DOI: 10.1016/j.watres.2012.10.026.

Boucher, J. and Friot, D. (2017). *Primary microplastics in the oceans: A global evaluation of sources*. Tech. rep.: 46. DOI: 10.2305/iucn.ch.2017.01.en.

Bradbury, S. and Evennett, P. J. (1996). *Contrast Techniques in Light Microscopy*. 1st ed. BIOS Scientific Publishers, Ltd.: 136.

Chapron, L., Peru, E., Engler, A., Ghiglione, J. F., Meistertzheim, A. L., Pruski, A. M., Purser, A., Vétion, G., Galand, P. E., and Lartaud, F. (2018). Macro- and microplastics affect cold-water corals growth, feeding and behaviour. *Scientific Reports* 8 (1): 1–8. DOI: 10.1038/s41598-018-33683-6.

Cox, K. D., Covernton, G. A., Davies, H. L., Dower, J. F., Juanes, F., and Dudas, S. E. (2019). Human Consumption of Microplastics. *Environmental Science & Technology*: 6. DOI: 10.1021/acs.est.9b01517.

Crittenden, J. C., Trussell, R. R., Hand, D. W., Howe, K. J., Tchobanoglous, G., and Borchardt, J. H. (2012). *MWH's Water Treatment Principles and Design*. 3rd ed.: 1901.

Eerkes-Medrano, D., Thompson, R. C., and Aldridge, D. C. (2015). Microplastics in freshwater systems: A review of the emerging threats, identification of knowledge gaps and prioritisation of research needs. *Water Research* 75: 63–82. DOI: 10.1016/j.watres.2015.02.012.

eKlima (2018). *Årsrapport - døgnverdier nedbør Ås*.

Enders, K., Lenz, R., Stedmon, C. A., and Nielsen, T. G. (2015). Abundance, size and polymer composition of marine microplastics >= 10 μm in the Atlantic Ocean and their modelled vertical distribution. *Marine pollution bulletin* 100 (1): 70–81.

Eriksen, M., Mason, S., Wilson, S., Box, C., Zellers, A., Edwards, W., Farley, H., and Amato, S. (2013). Microplastic pollution in the surface waters of the Laurentian Great Lakes. *Marine pollution bulletin* 77 (1-2): 177–182.

Erni-Cassola, G., Gibson, M. I., Thompson, R. C., and Christie-Oleza, J. A. (2017). Lost, but Found with Nile Red: A Novel Method for Detecting and Quantifying Small Microplastics (1 mm to 20 μm) in Environmental Samples. *Environmental Science and Technology* 51 (23): 13641–13648. DOI: 10.1021/acs.est.7b04512.

Friborg, T. (2015). Inaktivering av virus ved pasteurisering av svartvann fra Røde Kors' feltsykehus. PhD thesis: 106. URL: http://hdl.handle.net/11250/292934.

Fuentes, M. (2019). *Hemocytometer*. URL: https://www.hemocytometer.org/hemocytometer-protocol/.

Gall, S. C. and Thompson, R. C. (2015). The impact of debris on marine life. *Marine Pollution Bulletin* 92 (1-2): 170–179. DOI: 10.1016/j.marpolbul.2014.12.041.

GESAMP (2015). *Sources, fate and effects of microplastics in the marine environment: a global assessment*. Tech. rep.: 98.

GESAMP (2016). *Sources, fate and effects of microplastics in the marine environment: part two of a global assessment*. Tech. rep.: 96. URL: http://www.gesamp.org/publications/microplastics-in-the-marine-environment-part-2.

Greenspan, P., Mayer, E. P., and Fowler, S. D. (1985). Nile Red: A Selective Fluorescent stain for Intracellular Lipid Droplets. *The journal of cell biology* 100 (3): 965–973.

Gualtieri, M., Rigamonti, L., Galeotti, V., and Camatini, M. (2005). Toxicity of tire debris extracts on human lung cell line A549. *Toxicology in vitro* 19: 1001–1008. DOI: 10.1016/j.tiv.2005.06.038.

Haas, C. N., Rose, J. B., and Gerba, C. P. (1999). *Quantitative Microbial Risk Assessment, Second Edition*.

Hanke, G., Galgani, F., Werner, S., Oosterbaan, L., Nilsson, P., Fleet, D., Kinsey, S., Thompson, R., Palatinus, A., Van franeker, J. A., Vlachogianni, T., Scoullos, M., Veiga, J. M., Matiddi, M., Alcaro, L., Maes, T., Korpinen, S., Budziak, A., Leslie, H., Gago, J., and Liebezeit, G. (2013). *Guidance on Monitoring of Marine Litter in European Seas*. Publications Office of the European Union: 124. DOI: 10.2788/99475.

Helse- og omsorgsdepartementet (2017). *Forskrift om vannforsyning og drikkevann (drikkevannsforskriften)*.

Hidalgo-Ruz, V., Gutow, L., Thompson, R. C., and Thiel, M. (2012). Microplastics in the Marine Environment: A Review of the Methods Used for Identification and Quantification. *Environmental Science and Technology* 46: 3060–3075. DOI: 10.1021/es2031505.

Imhof, H. K., Schmid, J., Niessner, R., Ivleva, N. P., and Laforsch, C. (2012). A novel, highly efficient method for the separation and quantification of plastic particles in sediments of aquatic environments. *Limnology and Oceanography: Methods* 10: 524–537. DOI: 10.4319/lom.2012.10.524.

Imhof, H. K., Ivleva, N. P., Schmid, J., Niessner, R., and Laforsch, C. (2013). Contamination of beach sediments of a subalpine lake with microplastic particles. *Current Biology* 23 (19): R867–R868. DOI: 10.1016/j.cub.2013.09.001.

Introduksjon til Geoteknikk. *Emdal, A*: 187.

Jain, R., Mathur, M., Sikarwar, S., and Mittal, A. (2007). Removal of the hazardous dye rhodamine B through photocatalytic and adsorption treatments. *Journal of Environmental Management* 85 (4): 956–964. DOI: 10.1016/j.jenvman.2006.11.002.

Jan Kole, P., Löhr, A. J., Van Belleghem, F. G., and Ragas, A. M. (2017). Wear and tear of tyres: A stealthy source of microplastics in the environment. *International Journal of Environmental Research and Public Health* 14 (10): 31. DOI: 10.3390/ijerph14101265.

Karami, A., Golieskardi, A., Choo, C. K., Larat, V., Karbalaei, S., and Salamatinia, B. (2018). Microplastic and mesoplastic contamination in canned sardines and sprats. *Science of the Total Environment* 612: 1380–1386. DOI: 10.1016/j.scitotenv.2017.09.005.

Kayhanian, M., McKenzie, E. R., Leatherbarrow, J. E., and Young, T. M. (2012). Characteristics of road sediment fractionated particles captured from paved surfaces, surface run-off and detention basins. *Science of the Total Environment* 439: 172–186. DOI: 10.1016/j.scitotenv.2012.08.077.

Klein, J., Hulskotte, J., Ligterink, N., Dellaert, S., Molnàr, H., and Geilenkirchen, G. (2017). *Methods for calculating the emissions of transport in the Netherlands*. Tech. rep.: 74. URL: http://www.cbs.nl/NR/rdonlyres/2880AA1F-F077-45D2-94B5-7663A953EEF0/0/200611methodenrapportverkeereng.pdf.

Kosuth, M., Mason, S. A., and Wattenberg, E. V. (2018). Anthropogenic contamination of tap water, beer, and sea salt. *PLoS ONE* 13 (4): 18. DOI: 10.1371/journal.pone.0194970.

Kreider, M. L., Panko, J. M., McAtee, B. L., Sweet, L. I., and Finley, B. L. (2010). Physical and chemical characterization of tire-related particles: Comparison of particles generated using different methodologies. *Science of The Total Environment* 408 (3): 652–659. DOI: 10.1016/j.scitotenv.2009.10.016.

Lassen, C., Hansen, S. F., Magnusson, K., Hartmann, N. B., Rehne Jensen, P., Nielsen, T. G., and Brinch, A. (2015). *Microplastics Occurrence , effects and sources of releases*. Tech. rep. Ministry of Environment and Food: 208.

Le Pevelen, D. (2017). NIR FT-Raman. *Encyclopedia of Spectroscopy and Spectrometry*: 98–109. DOI: 10.1016/B978-0-12-409547-2.12150-X.

Li, S., Liu, H., Gao, R., Abdurahman, A., Dai, J., and Zeng, F. (2018). Aggregation kinetics of microplastics in aquatic environment: Complex roles of electrolytes, pH, and natural organic matter. *Environmental Pollution* 237: 126–132. DOI: 10.1016/j.envpol.2018.02.042.

Liebezeit, G. and Liebezeit, E. (2014). Synthetic particles as contaminants in German beers. *Food Additives and Contaminants: Part A* 31 (9): 1574–1578. DOI: 10.1080/19440049.2014.945099.

Luhana, L, Sokhi, R, Warner, L, Mao, H, Boulter, P, McCrae, I, Wright, J, and Osborn, D (2004). *Characterisation of Exhaust Particulate Emissions from Road Vehicles: Measurement of non-exhaust particulate matter*. Tech. rep.

Lusher, A. L., McHugh, M., and Thompson, R. C. (2013). Occurrence of microplastics in the gastrointestinal tract of pelagic and demersal fish from the English Channel. *Marine Pollution Bulletin* 67 (1-2): 94–99. DOI: 10.1016/j.marpolbul.2012.11.028.

Lusher, A. L., Buenaventura, N. T., Eidsvoll, D. P., Thrane, J.-E., Okelsrud, A., and Jartun, M. (2018). *Freshwater microplastics in Norway. A first look at sediment, biota and historical plankton samples from Lake Mjøsa and Lake Femunden*. Tech. rep.: 46.

Maes, T., Jessop, R., Wellner, N., Haupt, K., and Mayes, A. G. (2017). *A rapid-screening approach to detect and quantify microplastics based on fluorescent tagging with Nile Red*. DOI: 10.1038/srep44501.

Magnusson, K. (2014). *Mikroskräp i Avloppsvatten Från tre Norska Avloppsreningsverk*. Tech. rep. C 71. IVL Svenska Miljöinstitutet: 20.

Mantecca, P., Andrioletti, M., Gualtieri, M., Vismara, C., and Camatini, M. (2005). Impact of tire debris on in vitro and in vivo systems. *Particle and Fibre Toxicology* 2: 1–14. DOI: 10.1186/1743-8977-2-1.

Masliyah, J. (1998). Particle Deposition and Aggregation: Measurement, Modelling and Simulation. M. Elimelech et al. *Journal of Colloid and Interface Science - J COLLOID INTERFACE SCI* 200: 195. DOI: 10.1006/jcis.1997.5370.

Miljødirektoratet (2019). *Mikroplast*. URL: https://www.miljostatus.no/mikroplast.

Moody, V., Needles, H. L., Moody, V., and Needles, H. L. (2004). Fiber Identification and Characterization. *Tufted Carpet*: 23–34. DOI: 10.1016/B978-188420799-0.50003-8.

Moore, C. J. (2008). Synthetic polymers in the marine environment: A rapidly increasing, long-term threat. *Environmental Research* 108 (2): 131–139. DOI: 10.1016/j.envres.2008.07.025.

Murray, F. and Cowie, P. R. (2011). Plastic contamination in the decapod crustacean Nephrops norvegicus (Linnaeus, 1758). *Marine pollution bulletin* 62 (6): 1207–1217.

National Center for Biotechnology Information (2019a). *Nile red*. URL: https://pubchem.ncbi.nlm.nih.gov/compound/65182.

National Center for Biotechnology Information (2019b). *Rhodamine B*. URL: https://pubchem.ncbi.nlm.nih.gov/compound/rhodamine_b#section=Top.

Nerland, I.-L., Halsband, C., Allan, I., and Thomas, K. V. (2014). *Microplastics in marine environments: Occurrence, distribution and effects*. Tech. rep.: 71. DOI: 10.1183/09031936.06.00108105.

NIVA (2017). *EU Water Framework Directive*. URL: https://www.niva.no/en/services/eu-water-framework-directive.

Ødegard, H., Lindholm, O., Østerhus, S. W., Thorolfsson, S. T., Sægrov, S., Mosevoll, G., and Heistad, A. (2014). *Vann- og avløpsteknikk*. 2nd ed. Norsk Vann: 664.

Pearson Correlation Coefficient Calculator (2019). URL: https://www.socscistatistics.com/tests/pearson/default2.aspx.

Richardson, S. D., Willson, C. S., and Rusch, K. A. (2004). Use of Rhodamine Water Tracer in the Marshland Upwelling System. *Ground Water* 42 (5): 678–688.

Rumin, J., Bonnefond, H., Saint-Jean, B., Rouxel, C., Sciandra, A., Bernard, O., Cadoret, J. P., and Bougaran, G. (2015). The use of fluorescent Nile red and BODIPY for lipid measurement in microalgae. *Biotechnology for Biofuels* 8 (1): 16. DOI: 10.1186/s13068-015-0220-4.

Sanchez, W., Bender, C., and Porcher, J. M. (2014). Wild gudgeons (Gobio gobio) from French rivers are contaminated by microplastics: Preliminary study and first evidence. *Environmental Research, Elsevier* 128: 14. DOI: 10.1016/j.envres.2013.11.004.

Schymanski, D., Goldbeck, C., Humpf, H. U., and Fürst, P. (2018). Analysis of microplastics in water by micro-Raman spectroscopy: Release of plastic particles from different packaging into mineral water. *Water Research* 129: 154–162. DOI: 10.1016/j.watres.2017.11.011.

Shim, W. J., Song, Y. K., Hong, S. H., and Jang, M. (2016). Identification and quantification of microplastics using Nile Red staining. *Marine Pollution Bulletin* 113 (1-2): 8. DOI: 10.1016/j.marpolbul.2016.10.049.

Snilsberg, B. (2008). Pavement wear and airborne dust pollution in Norway- Characterization of the physical and chemical properties of dust particles. PhD thesis. Norwegian University of Science and Technology: 133.

Statens vegvesen (2010). *Geoteknikk i vegbygging(V220)*. Håndbok: 73. URL: https://www.vegvesen.no/_attachment/70057/binary/1305835?fast_title=HÃ¥ndbok+V220+Geoteknikk+i+vegbygging+%2818+MB%29.pdf.

Statens Vegvesen (2014). *Håndbok N200 Vegbygging*: 148–150. URL: https://www.vegvesen.no/_attachment/188382/binary/980128?fast_title=HÃ¥ndbok+N200+Vegbygging+(21+MB).pdf.

Statens vegvesen (2018a). *Annual average daily traffic, Drobakveien*. URL: https://www.vegvesen.no/vegkart/vegkart/#kartlag:geodata/hva:(~(farge:'0_0,id:540))/@263074,6621771,14/vegobjekt:83258556:40a744:540.

Statens vegvesen (2018b). *Vegbygging(N200)*: 98–101.

Sundt, P., Schulze, P.-E., and Syversen, F. (2014). Sources of microplastic- pollution to the marine environment. *Mepex for the Norwegian Environment Agency*: 86.

Syversen, F (1989). *Brukte bildekk I Norge – problemer og muligheter*. Tech. rep. SFT/Berdal Strømme Rapport.

Thompson, R. C., Olsen, Y., Mitchell, R. P., Davis, A., Rowland, S. J., John, A. W. G., McGonigle, D., and Russell, A. E. (2004). Lost at sea: where is all the plastic? *Science* 304 (5672): 2.

Thompson, R. C., Moore, C. J., vom Saal, F. S., and Swan, S. H. (2009). Plastics, the environment and human health: Current consensus and future trends. *Philosophical Transactions of the Royal Society B: Biological Sciences* 364 (1526): 2153–2166. DOI: 10.1098/rstb.2009.0053.

UNECE (2013). *Particulate Matter Emissions by Tyres*.

Van Cauwenberghe, L. and Janssen, C. R. (2014). Microplastics in bivalves cultured for human consumption. *Environmental Pollution* 193: 65–70. DOI: 10.1016/j.envpol.2014.06.010.

Verschoor, A. (2015). *Towards a definition of microplastics- Considerations for the specification of physico-chemical properties*. Tech. rep.: 38. URL: https://rivm.openrepository.com/bitstream/handle/10029/575986/2015-0116.pdf;jsessionid=68A2105D4B455E27F57A64A5A08D26A2?sequence=3.

Verwey, E., Overbeek, J., and Van Nes, K. (1948). *Theory of the Stability of Lyophobic Colloids: The Interaction of Sol Particles Having an Electric Double Layer*: 205.

Vogelsang, C., Lusher, A. L., Dadkhah, M. E., Sundvor, I., Umar, M., Ranneklev, S. B., Eidsvoll, D., and Meland, S. (2018). *Microplastics in road dust – characteristics, pathways and measures*. Tech. rep.: 171. URL: https://brage.bibsys.no/xmlui/handle/11250/2493537.

Wagner, M., Scherer, C., Alvarez-Muñoz, D., Brennholt, N., Bourrain, X., Buchinger, S., Fries, E., Grosbois, C., Klasmeier, J., Marti, T., Rodriguez-Mozaz, S., Urbatzka, R., Vethaak, A. D., Winther-Nielsen, M., and Reifferscheid, G. (2014). Microplastics in freshwater ecosystems: what we know and what we need to know. *Environmental Sciences Europe* 26 (1): 9. DOI: 10.1186/s12302-014-0012-7.

Webster, D. R. and Weissburg, M. J. (2009). The Hydrodynamics of Chemical Cues Among Aquatic Organisms. *Annual Review of Fluid Mechanics* 41 (1): 73–90. DOI: 10.1146/annurev.fluid.010908.165240.

Wiesner, M. R. and Bottero, J.-Y. (2007). *Environmental Nanotechnology: Applications and Impacts of Nanomaterials*. 1st ed. McGraw-Hill Education: New York: 416.

Wik, A. and Dave, G. (2006). Acute toxicity of leachates of tire wear material to Daphnia magna-Variability and toxic components. *Chemosphere* 64: 1777–1784. DOI: 10.1016/j.chemosphere.2005.12.045.

Wright, S. L. and Kelly, F. J. (2017). Plastic and Human Health: A Micro Issue? *Environmental Science and Technology* 51 (12): 6634–6647. DOI: 10.1021/acs.est.7b00423.

Wright, S. L., Rowe, D., Thompson, R. C., and Galloway, T. S. (2013a). Microplastic ingestion decreases energy reserves in marine worms. *Current Biology* 23 (23): R1031–R1033. DOI: 10.1016/j.cub.2013.10.068.

Wright, S. L., Thompson, R. C., and Galloway, T. S. (2013b). The physical impacts of microplastics on marine organisms: a review. *Environmental pollution* 178: 483–492. DOI: 10.1016/j.envpol.2013.02.031.

Appendix A. Calculations for particle size distribution

Table A.1: Calculations for particle size distribution for sample 1.

Wet sample (g)	Dry sample (g)				
20,012	16,866				
Mesh width	Container (g)	Container + dry sample (g)	Dry sample (g)	Dry sample (%)	d_n
2 mm	24,556	25,952	1,396	8,277	91,723
600 µm	25,142	28,535	3,393	20,118	71,605
212 µm	23,253	29,502	6,249	37,051	34,554
63 µm	23,971	26,432	2,461	14,592	19,962
20 µm	46,738	48,319	1,581	9,374	10,588
Sum:			15,080	89,412	

CORRECTION FACTOR	
Container (g):	12,875
Container + wet sample (g):	14,885
Wet sample (g):	2,010
Container + dry sample (g):	14,569
Dry sample (g):	1,694
Correction factor (dry/wet):	**0,843**

Table A.2: Calculations for particle size distribution for sample 2.

Wet sample (g)	Dry sample (g)				
20,036	15,844				
Mesh width	Container (g)	Container + dry sample (g)	Dry sample (g)	Dry sample (%)	d_n
2 mm	16,882	21,172	4,290	27,076	72,924
600 µm	18,630	19,964	1,334	8,420	64,504
212 µm	20,386	23,062	2,676	16,890	47,614
63 µm	20,355	23,418	3,063	19,332	28,282
20 µm	48,730	51,274	2,544	16,057	12,226
Sum			13,91	87,77	

CORRECTION FACTOR	
Container (g):	13,178
Container + wet sample (g):	15,195
Wet sample (g):	2,017
Container + dry sample (g):	14,773
Dry sample (g):	1,595
Correction factor (dry/wet):	**0,791**

Table A.3: Calculations for particle size distribution for sample 3.

Wet sample (g)	Dry sample (g)				
20,063	17,256				
Mesh width	Container (g)	Container + dry sample (g)	Dry sample (g)	Dry sample (%)	d_n
2 mm	20,450	21,966	1,516	8,786	91,214
600 µm	19,809	20,750	0,941	5,453	85,761
212 µm	20,429	21,556	1,127	6,531	79,230
63 µm	19,462	21,589	2,127	12,326	66,903
20 µm	44,110	47,146	3,036	17,594	49,309
Sum			8,75	50,69	

CORRECTION FACTOR	
Container (g):	13,350
Container + wet sample (g):	15,401
Wet sample (g):	2,051
Container + dry sample (g):	15,114
Dry sample (g):	1,764
Correction factor (dry/wet):	**0,860**

Table A.4: Calculations for particle size distribution for materials donated by Franzefoss Pukk.

Dry sample (g)					
20,007					
Mesh width	Container (g)	Container + dry sample (g)	Dry sample (g)	Dry sample (%)	d_n
2 mm	19,407	24,404	4,997	24,976	75,024
600 µm	15,877	23,428	7,551	37,742	37,282
212 µm	17,792	21,437	3,645	18,219	19,063
63 µm	19,983	22,283	2,300	11,496	7,567
20 µm	44,365	45,725	1,360	6,798	0,770
Sum			19,85	99,23	

Table A.5: Calculations for new particle size distribution for the materials according to the NPRA.

Dry sample (g)			
100,000			
Mesh width	d_n	Dry sample (%)	Dry sample (g)
212 µm	60,000	40,000	40,000
63 µm	30,000	30,000	30,000
20 µm	0,000	30,000	30,000
Sum		100,00	100,00

Appendix B. Calculations for particle concentrations, particle reduction and filter coefficients

Table B.1: Number of particles per square in hemocytometer, average particle per square for each sample, concentration of particle/ml for each sample, log reduction and percentage reduction.

Square nr.	**Method**	**$C_0$1**	**1.1**	**1.2**	**1.3**	**2.1**	**2.2**	**2.3**
1		40	0	0	0	5	3	1
2		55	0	1	0	0	0	0
3		25	0	0	0	0	0	1
4		25	0	3	0	1	6	0
5		42	0	0	0	1	0	0
6		38	0	1	0	0	0	0
7		27	1	0	0	0	1	1
8		30	0	4	0	1	0	0
9		76	0	1	0	0	0	0
10		30	0	0	0	1	3	5
11		17	0	0	0	0	0	4
12		29	1	0	0	0	1	0
13		5	0	0	0	2	0	0
14		18	2	1	0	0	0	0
15		15	0	0	0	0	0	0
16		17	0	1	0	0	0	0
17		64	0	0	0	1	1	0
18		25	0	0	0	0	0	2
19		26	1	1	0	0	0	2
20		5	1	5	0	2	0	3
Average/square:	Counted	30.45	0.3	0.9	0	0.7	0.75	0.95
Particle/ml:	Avrg · vol. of square	7 612 500	75 000	225 000	37400*	175 000	187 500	237 500
Volume (ml):	From Table 3.1	2 058	343	343	343	343	343	343
Total particles out:	Part/ml · volume	-	2,573E+07	7,718E+07	1,283E+07	6,003E+07	6,431E+07	8,146E+07
Total particles in:	Part/ml · volume	1,567E+10	2,611E+09	2,611E+09	2,611E+09	2,611E+09	2,611E+09	2,611E+09
Log-reduction:	Log(part.in/part.out)	-	2.006	1.529	2.309	1.638	1.609	1.506
Reduction (%):	$(1-\frac{\text{part.out}}{\text{part.in}})\cdot 100\%$	-	99.015	97.0443	99.509	97.701	97.537	96.880

* Particle per ml from equation 4.1.

Table B.2: Number of particles per square in hemocytometer, average particle per square for each sample, concentration of particle/ml for each sample, log reduction and percentage reduction.

Square nr.	Method	$C_0.2$	3.2	3.3	$C_0.3$	4.1	4.2	4.3
1		5	0	3	15	0	0	0
2		10	0	0	17	0	0	0
3		9	0	0	12	0	0	0
4		13	0	0	28	0	0	0
5		21	1	0	17	0	0	0
6		18	0	0	23	0	0	0
7		22	0	0	16	0	0	0
8		16	0	0	26	0	0	0
9		19	0	0	33	0	0	0
10		17	2	0	5	0	0	0
11		30	1	0	13	0	0	0
12		22	3	0	26	0	0	0
13		20	1	0	16	0	0	0
14		14	2	0	11	0	0	0
15		11	0	0	19	0	0	0
16		27	2	0	32	0	0	0
17		5	1	0	27	0	0	0
18		20	0	0	17	0	0	0
19		32	0	0	12	0	0	0
20		22	1	0	32	0	0	0
Average/square:	Counted	17.65	0.7	0.15	19.85	0,00	0,00	0,00
Particle/ml:	Avrg · vol. of square	4 412 500	175 000	37 500	4 962 500	37400*	37400*	37400*
Volume (ml):	From Table 3.2,3.3	688,00	344,00	344,00	2 021,00	505.25	505.25	505.25
Total particles out:	Part/ml · volume	-	6,020E+07	1,290E+07	-	1,890E+07	1,890E+07	1,890E+07
Total particles in:	Part/ml · volume	3,036E+09	1,518E+09	1,518E+09	1,003E+10	2,507E+09	2,507E+09	2,507E+09
Log-removal:	Log(part.in/part.out)	-	1.402	2.071	-	2.123	2.123	2.123
Reduction (%):	$(1-\frac{\text{part.out}}{\text{part.in}})\cdot 100\%$	-	96.034	99.150	-	99.246	99.246	99.246

* Particle per ml from equation 4.1.

Table B.3: Calculations for filter coefficients.

	Method	1.1	1.2	1.3	2.1	2.2	2.3	3.2	3.3	4.1	4.2	4.3
Total particles out:	Calculated	2,57E+07	7,72E+07	3,74E+04	6,00E+07	6,43E+07	8,15E+07	6,02E+07	1,29E+07	3,74E+04	3,74E+04	3,74E+04
Total particles in:	Calculated	2,61E+09	2,61E+09	2,61E+09	2,61E+09	2,61E+09	2,61E+09	1,52E+09	1,52E+09	2,51E+09	2,51E+09	2,51E+09
Filter depth (m):	Measured *	0,107	0,07	0,143	0,066	0,076	0,073	0,081	0,076	0,13	0,126	0,083
Filter coefficient (m^{-1})	$\frac{1}{L}*\ln(\frac{\text{part. in}}{\text{part. ut}})$	43.178	50.306	77.997	57.163	48.734	47.498	39.845	62.735	85.485	88.199	133.892

* From tables 3.1, 3.2 and 3.3

Appendix C. Calculations for correlations

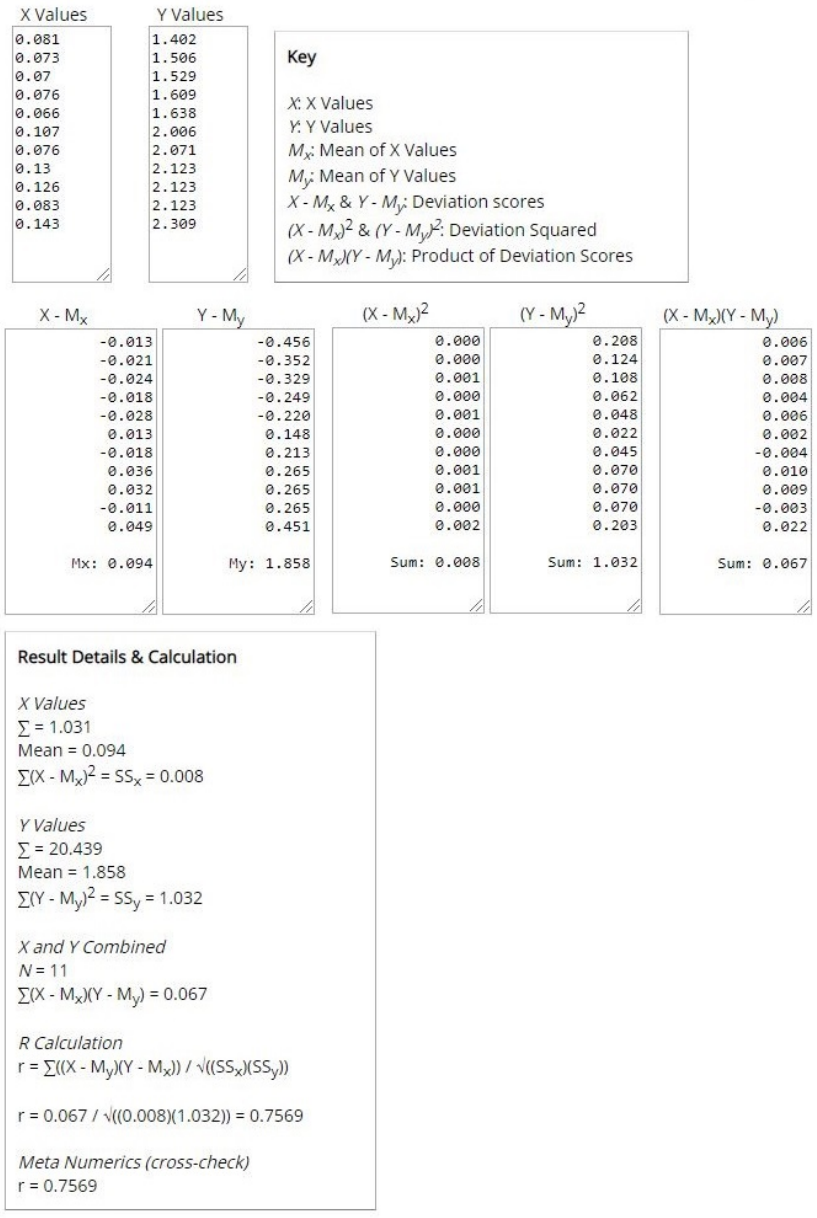

Figure C.1: Calculations for correlation of log reduction and filter depth (*Pearson Correlation Coefficient Calculator* 2019).

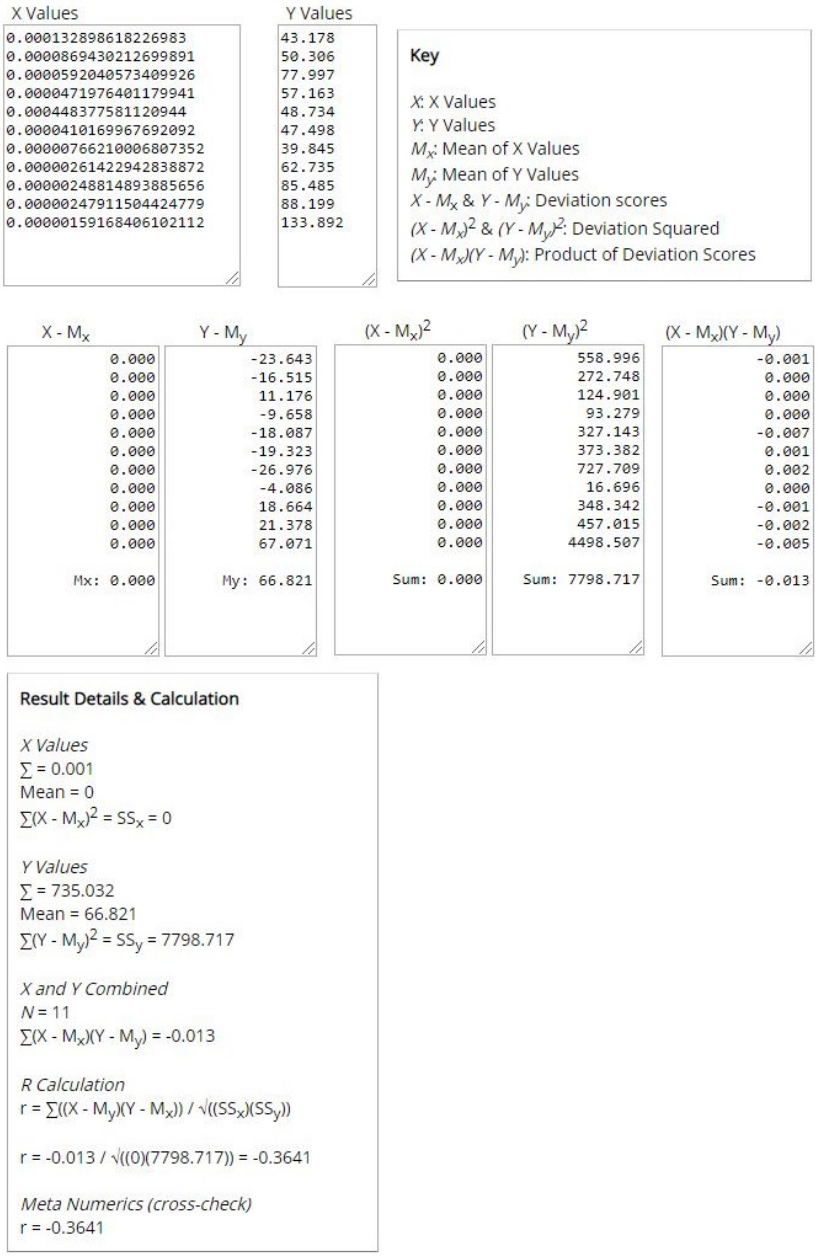

Figure C.2: Calculations for correlation of filter coefficient and hydraulic conductivity (*Pearson Correlation Coefficient Calculator* 2019).

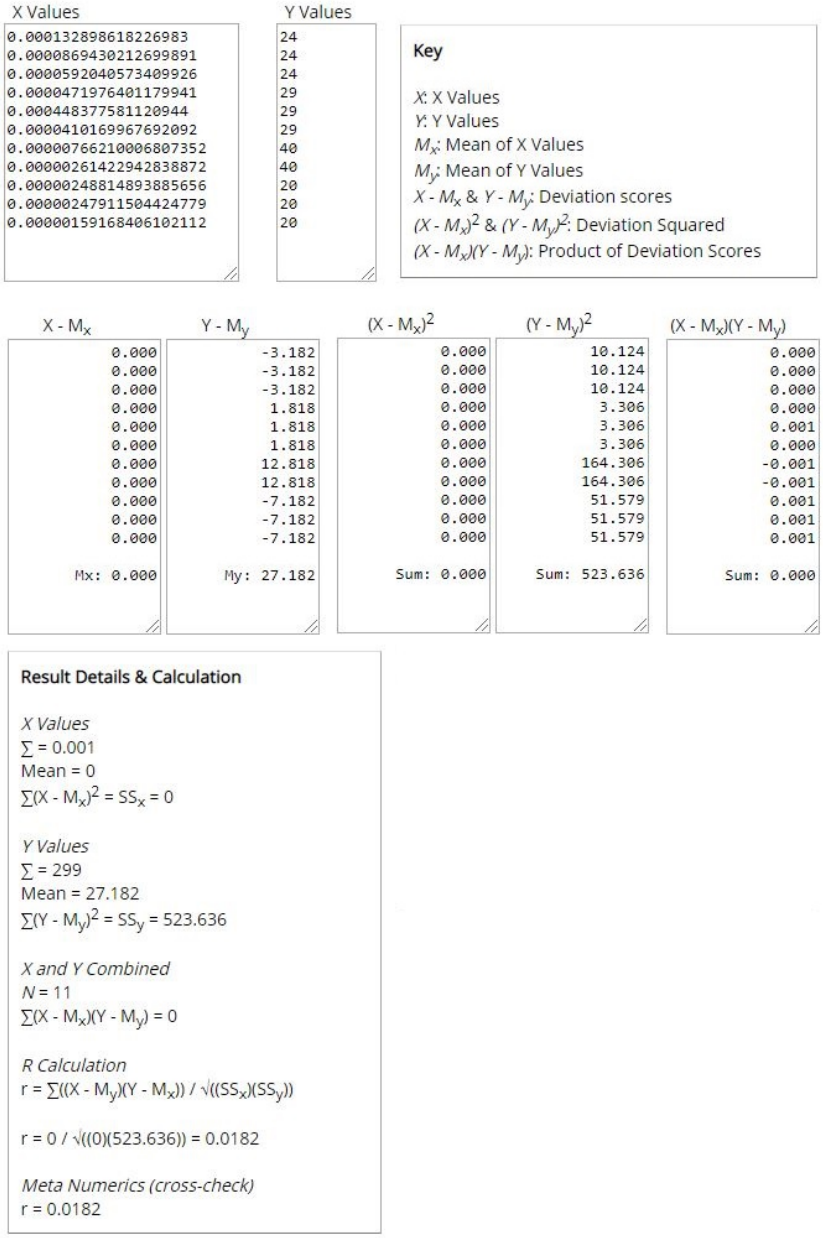

Figure C.3: Calculations for correlation of uniformity coefficient and hydraulic conductivity (*Pearson Correlation Coefficient Calculator* 2019).

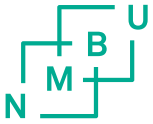

Norges miljø- og biovitenskapelige universitet
Noregs miljø- og biovitskapelege universitet
Norwegian University of Life Sciences

Postboks 5003
NO-1432 Ås
Norway